AD NUMBER

ADB193430

NEW LIMITATION CHANGE

TO

Approved for public release, distribution unlimited

FROM

Distribution authorized to U.S. Gov't. agencies and their contractors; Administrative/Operational Use; 28 SEP 1961. Other requests shall be referred to National Aeronautics and Space Administration, Langley Research Center, Hampton, VA.

AUTHORITY

NASA TR Server Website

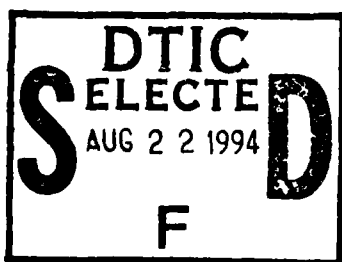1D

AD-B193 430

COPY 1

N-99819

ENGINEERING ASPECTS OF FATIGUE CRACK PROPAGATION

By Herbert F. Hardrath and Arthur J. McEvily, Jr.

Langley Research Center
Langley Air Force Base, Va., U.S.A.

For Presentation at a Symposium
on Crack Propagation

Cranfield, England
September 26-28, 1961

94-26247

ACKNOWLEDGEMENTS

ENGINEERING ASPECTS OF FATIGUE CRACK PROPAGATION

By Herbert F. Hardrath[*] and Arthur J. McEvily, Jr.[**]

INTRODUCTION

Fatigue crack propagation is a complex process which has been the subject of much study during recent years. It is of concern to people with a wide range of interests. Solid state physicists and metallurgists study the movement of dislocations to initiate the crack and the factors affecting propagation on a microscopic scale. Those who endeavor to understand and predict fatigue behavior from a phenomenological point of view find it an important factor in the study of cumulative damage. Designers of machines and structures need information on crack propagation and its effects in order to provide materials and configurations which either do not experience fatigue failure or which maintain a high level of residual strength and a low rate of crack propagation. Operators of such machines must have information on crack propagation in order to develop regular inspection schedules to detect cracks before catastrophic failure occurs.

At the Langley Research Center of the National Aeronautics and Space Administration a number of investigations have been carried out to study various phases of the phenomenon. It is the purpose of this paper to review those portions of the work which have revealed important factors

---

[*]Head, Fatigue Branch, NASA Langley Research Center, Langley Air Force Base, Virginia.

[**]Formerly Head, Solid State Physics Section, NASA Langley Research Center, Langley Air Force Base, Virginia, now with the Scientific Laboratory, Ford Motor Co., Dearborn, Michigan.

L-1709

governing the phenomenon and to present an engineering approach to pre-
dicting the rate of crack propagation. This method, which is closely
related to methods of analysis useful for correlating fatigue notch
sensitivity and residual static strength in parts containing fatigue
cracks, will be used to correlate the results of a variety of tests of
simple specimens made of structural materials.

The present state of knowledge of the basic mechanism will be
reviewed before the computational details are presented. Metallurgical
factors will also be discussed. The factors governing crack growth in
complex structures will be considered and a comparison with crack growth
in simple specimens will be made.

THE PROCESS OF FATIGUE CRACK GROWTH

Fatigue cracks are usually formed within glide bands, frequently
very early in life. Such cracks are usually isolated within single
grains of a polycrystal and can remain and grow in these grains for a
considerable portion of the life of a specimen. Such processes as cross
slip and the formation of extrusions and intrusions are associated with
this stage of crack development.

At a later stage individual cracks coalesce and propagate macro-
scopically across many grains. This macroscopic growth is more or less
in a plane normal to the principal tensile stress although within indi-
vidual grains the path may be along crystallographic planes and may
involve such processes as cross slip (refs. 1 to 2). Tests have shown
(ref. 3) that visible cracks can be present for 50 percent or more of
the fatigue life. This is especially true in notched parts, as can be

explained by comparing the failure of notched and unnotched specimens

having equal lives. The notched specimen is, of course, stressed at a

lower level than the unnotched; thus, a longer crack must form in the

notched than in the unnotched specimen before failure occurs. Furthermore,

the rate of crack propagation is lower in the notched specimen than in the

unnotched because lower stresses are operating. Both of these factors,

longer crack growth and lower driving stress, contribute to long periods

of crack growth. In view of the fact that practical structures inevitably

contain discontinuities, macroscopic crack growth is a very important part

of the life of a structure. Cracks detected during this phase serve to

warn the operator of impending danger of catastrophic failure. Because

of the engineering significance of this portion of crack growth, it will

be the primary concern of this paper.

The work of Head (ref. 4) is typical of early interpretations of

the macroscopic crack propagation process. He envisioned growth to occur

in two steps. During the first step the crack was stationary while a

small volume of material just ahead of the crack was hardened by succes-

sive stress cycles until it failed as in the Orowan (ref. 5) mechanism.

In the second step the crack moved forward an incremental distance until

it was arrested in more ductile material ahead of the crack.

The electron microscope studies of Forsyth and Ryder (ref. 6) verify

that, at low stress levels, fatigue cracks propagate in two steps, but

that the first stage differs from that visualized by Head. These studies

have shown that some crack growth occurs in each cycle and that the shape

of the crack front is an important factor in the propagation process.

The schematic representation of a fatigue fracture surface in figure 1

indicates the sequence of events which takes place. Forsyth and Ryder found that fatigue cracks tend to grow deeper at the midplane of a sheet specimen than at the surface and that fracture surfaces are often alternately dull and bright even in tests under a constant amplitude of stress. The dull regions are very much like static tensile failures and, indeed, are produced by sudden bursts of crack growth. Such growth is caused by a triaxial state of stress ahead of the crack and is brittle in the sense that crack growth is rapid and there is little accompanying plastic deformation. After such a burst the material at the trailing edge of the crack tends to be very highly stressed. Thus, growth is encouraged in the material near the surface. This growth is mostly by shear and produces a bright band on the fracture surface. Much less growth occurs at the interior because as in static failure (ref. 7) the material near the surface of the specimen keeps the crack from opening and limits the stress in the interior. When sufficient crack growth has occurred at the surface to allow increased deformation and stress at the center, another sudden burst of growth in the interior occurs, and the two-stage process is repeated. As growth continues the crack length at the interior exceeds that at the surface by increasing amounts. The amount by which the crack "tunnels" into the interior also increases with the applied stress.

The fact that cracks advance in practically every cycle indicates that material near the crack front is experiencing changes which make that material vulnerable to failure while other material farther from the crack is less affected. The schematic stress-strain diagram in figure 2 illustrates the action at the crack tip. Assume that the point

labelled 1 represents the stress state near the trailing edge of the crack immediately after an increment of crack growth. As the specimen is unloaded the crack tends to close. Depending on the mean load and the local stress conditions, reversed plastic strain may take place and the point 2 is reached. Upon reloading, the local stress increases and an increment of plastic flow is again produced. Since the material under consideration was on the verge of fracture in the previous cycle, it is considered that only a slight additional plastic strain is sufficient to precipitate local fracture. Some unpublished work by McEvily with single crystals of lithium fluoride at large strains has shown that the set of slip planes active during compression loading is different from the set active during tension loading. Thus, the compression load does not relieve to any appreciable extent the systems operating during tension loading. The crack advances through the region where the total allowable forward-direction plastic strain has been exceeded and then stops in material that has not been worked as severely. The process is repeated in succeeding loading cycles until conditions in the interior of the specimen produce a sudden burst of crack growth there.

The foregoing observations apply where cracks grow at high stresses and in thick specimens when crack growth is roughly in a plane at 90° to the applied stress. In thin sheet specimens the brittle burst stage may be minimized because the amount of triaxiality which can be developed is limited. In these cases the crack usually shifts to a plane at 45° to the surface of the specimen during later stages of crack growth. The tendency for initial growth at 90° to the principal tension stress is very strong. Frost and Dugdale (ref. 8) showed that cracks grew at 90°

even when sharp notches were introduced to encourage initial propogation at 45°.

Investigators disagree on whether the overall rate of crack growth changes significantly and abruptly (refs. 9 to 12) when the crack shifts to the 45° plane in tests with constant-amplitude loading. Some of the disagreement may stem from the frequency of making measurements, the kind of material tested, the loading conditions used, the kinds of diagrams which are drawn to depict the phenomenon, and the individual interpretation made by the investigators. Any rapid increase in observed rate of crack growth is not necessarily attributable to crack growth on a 45° plane.

Static tests of 7075-T6 aluminum-alloy sheet specimens with sharp notches cut at 45° to the plane of the sheet have shown that the stress level at which cracks formed and began to propagate slowly was essentially the same as that at which the same action took place when notches were cut normal to the plane of the specimen. The crack undoubtedly progresses along whatever plane responds more readily to the stresses present. At e time of the gradual shift to the 45° plane, the stress systems tending to produce crack extension along 90° or 45° planes must be very nearly the same. Thus the transition from one plane to another is gradual. As will be seen in later sections of this paper, the progressive increase in rate of crack propagation can be explained by considerations of the progressive increase in local stress.

METHOD FOR CORRELATING RATE OF CRACK PROPAGATION

From the foregoing discussion it is evident that the state of stress at the crack front is a most important factor governing the rate of crack propagation. Thus, methods for correlating and predicting rates of growth must consider the local stress. It is reasonable to expect that cracks in different specimens of the same material should grow at equal rates if the local stress states are the same. Another factor of importance is the magnitude of local stresses compared with the minimum stress required to propagate the fatigue crack. Many investigators interpret the stress required to propagate an embryonic fatigue crack to be the true fatigue limit of a material (refs. 1, 13, and 14). A method for correlation and prediction of crack growth in simple specimens has been developed which is based on considerations of local stress at the crack tip. This method will now be discussed.

The computation of the true local stress at the crack tip is rather complicated because of the plastic deformations which occur at the crack front and because of extremely steep stress gradients encountered around cracks. In order to simplify the procedure it was decided to base the correlation procedure on stresses computed with elastic considerations. The local stress will be determined from the local stress concentration factor and the average stress applied to the remaining cross section of the specimen.

To compute the stress concentration factor at a discontinuity, two parameters concerning the configuration must be known. One parameter which must be defined is the size of the discontinuity relative to other

dimensions of the specimen. This parameter is generally well defined and numerous analytical procedures for computing stress concentrations are available. Typical of these are works by Howland (ref. 15) for holes concentrically located in axially loaded strips, an extension to nonsymmetrical cases by Sjostrom (ref. 16) and Neuber's (ref. 17) treatment of a variety of internal and external notches. The other, and probably more important, parameter is the radius of curvature at the point of maximum stress. In the case of cracks, this dimension is generally not known but must be very small.

A convenient procedure for analysis of stresses around very sharp notches has been developed by Neuber (ref. 17). In the development of his technical factor, Neuber recognizes that, as the notch radius approaches dimensions of the order of the grain size, the behavior of materials departs from the homogeneous and isotropic behavior assumed in the theory of elasticity. To account for this he assumes that stresses within some finite volume of material are undetermined and that the actual maximum stress at a sharp discontinuity approaches a limiting

value which would be computed if the notch radius were equal to the radius of this volume. He called this small volume a "building block" and its characteristic radius was designated ρ'. The dimension ρ' is considered to be a property of the material, but must be adjusted empirically to fit experimental results.

The Neuber technical factor has been applied by Kuhn and Hardrath (ref. 18) to account for the well-known fatigue notch-size effect. An example of this effect is shown in figure 3 where the effective stress concentration factor K_F observed in tests of geometrically similar

- 8 -

specimens is plotted against the radius of curvature ρ in the notch. In this particular example aluminum-alloy sheet specimens with holes were tested (ref. 19) under completely reversed axial loads. The data for three sizes of specimens indicate that K_F decreases with decreasing size, but the elastic stress concentration factor K_T remains constant.

Kuhn and Hardrath found that good correlation of a variety of such results of tests on steels was achieved when the value ρ' was varied with the ultimate tensile strengths of the steels involved. Further analysis indicates that a similar correlation may be realized for aluminum alloys. Although no direct correlation has been found between ρ' and the grain size, the trend in values of ρ' is consistent with that of the probable grain size.

A further adaptation of the Neuber technical factor was made by McEvily, Illg, and Hardrath (ref. 20) in the analysis of the residual static strength of specimens containing fatigue cracks. For this analysis, a system was developed for computing elastic stress concentration factors for cracks of various lengths. An effective radius of curvature ρ_e at the crack tip and the Neuber constant ρ' were adopted to compute an elastic stress concentration factor. A correction was made to account for plastic effects and failure was assumed to occur when the maximum local stress reached the ultimate tensile strength of the material.

In the analysis of residual static strengths in aluminum alloy it was found that the effective radius of curvature ρ_e and the Neuber constant ρ' were approximately equal to each other and were of the order of 0.003 inch.

- 9 -

The procedure adopted for calculation of stress concentration factors for the present purpose is essentially the same as that developed in reference 20. An example of this calculation procedure follows. Figure 4 shows a sheet specimen containing a central hole with cracks growing from each side. The first step in the computation is based on an adaptation of Howland's solution for a central hole. The hole is assumed to have a diameter equal to twice the length of the crack, including the initial hole. The Howland solution yields stress concentrations K_c (fig. 5) ranging from 3 for very small holes to 2 for large holes. This solution is modified to account for the fact that the crack is more nearly an elongated ellipse by the formula

$$K_e = 1 + (K_c - 1)\sqrt{\frac{l}{\rho_e}}$$

where K_e is the stress concentration factor for an ellipse with semi-major axis l and root radius ρ_e. The factor $\sqrt{\frac{l}{\rho_e}}$, in which l is the half-length of the crack and ρ_e is the effective radius of curvature at the crack tip, yields the appropriate solution for a circular hole when $l = \rho_e$ and agrees with Neuber's solution (ref. 14) for stress concentrations at an ellipse in an infinite sheet. At this point the solution is modified to account for the notch-size effect treated in Neuber's technical factor:

$$K_N = 1 + \frac{K_e - 1}{1 + \sqrt{\frac{\rho'}{\rho_e}}}$$

- 10 -

The assumption that $\rho' = \rho_e$ allows the simplification of the K_N equation to: $K_N = 1 + \frac{1}{2}(K_c - 1)\,\frac{l}{\rho_e}$. For high strength steels, however, this simplification does not appear appropriate and ρ_e and ρ' sometimes require separate empirical adjustment.

For the aluminum alloys, for which $\rho' \approx \rho_e$, the determination of ρ_e is made as follows. It is assumed that cracks will propagate whenever the product of the Neuber technical factor K_N and the stress on the remaining section S_{NET} exceeds the fatigue limit S_f for unnotched specimens of the same material tested at the same ratio of minimum to maximum cyclic load. The minimum value of $K_N S_{NET}$ required to propagate a crack is determined experimentally. This value can be found with a reasonable effort by conducting a test in which the applied load is decreased progressively by small increments until the crack no longer propagates. The value of ρ_e is then computed from the relation

$$S_f = S_{NET}\left[1 + \frac{1}{2}(K_c - 1)\,\frac{l}{\rho_e}\right]$$

in which ρ_e is the only unknown.

As indicated earlier, the rate of crack propagation might be expected to be equal in specimens having the same local stress regardless of the applied load or crack length. The parameter $K_N S_{NET}$ represents this local stress and should provide a means for correlating rates of crack growth. Also, the relation $K_N S_{NET} = S_f$ should become a governing criterion by which to identify propagating or nonpropagating cracks.

- 11 -

For a critical test of this hypothesis, specimens of various sizes containing cracks of various lengths should be tested at a variety of applied loads. The following sections of the paper will present such data and an evaluation of the method just described.

COMPARISON WITH EXPERIMENTAL DATA

In order to check the adequacy of the method outlined, data from NASA and other investigations have been analyzed. Some of these analyses will be discussed in this section of the paper. In figures 6 and 7 are plotted the results of axial load fatigue tests (ref. 21) of 2024-T3 and 7075-T6 aluminum-alloy sheet specimens. Specimens were 2 inches and 12 inches wide and all loadings had a ratio R of minimum to maximum cyclic stress of zero. The rate of crack propagation is plotted against the parameter $K_N S_{NET}$ in which K_N was computed with values of $\rho_e = \rho'$ equal to 0.002 inch for the aluminum-zinc-magnesium alloy (7075-T6) and 0.003 inch for the aluminum-copper alloy (2024-T3). These values of ρ_e were established in tests which determined the minimum stress to propagate cracks. Both K_N and S_{NET} increase steadily as the crack grows, thus the results of each test appear as a continuous curve. The results of all tests for a given material fall within a reasonably narrow scatter band despite differences in width, crack length, and stress level. This suggests the establishment of a "master curve" for predicting all the results shown.

Such a curve has been fitted to the data and appears, together with its equation, in figures 6 and 7. The curve has been adjusted to approac'

- 12 -

zero rate of crack growth as the product $K_N S_{NET}$ approaches 34 ksi, a

value which is a good estimate of the minimum stress required to produce

failure in unnotched specimens of each of these same materials tested

under repeated axial loads with $R = 0$ (ref. 22). Although good correla-

tion was looked for on the basis of the foregoing discussion, there was

no reason to expect that the same equation would serve to correlate the

results of the two materials. This part of the result appears to be a

coincidence.

A similar set of results (ref. 23) was obtained for tests of 12-inch-

wide specimens made of the same materials as before but under completely

reversed loads $(R = -1)$. These results are presented in figure 8. The

values of K_N were computed for the same values of ρ_e as were used

for $R = 0$ tests. Here again, the data fall in a reasonably narrow

scatter band for each material. A good fit of the data is obtained by

an equation similar to that used before except that the minimum stress

to propagate a crack was changed to 20 ksi, a value which agrees with

tests of unnotched specimens of these materials at $R = -1$ (ref. 22).

Except for the lower limiting stress the equation given for results of

tests of 7075-T6 follows very nearly the same curve as that used in fig-

ure 7 for tests at $R = 0$. This result indicates that, in this material

at least, the rate of crack propagation is dependent primarily on the

maximum cyclic stress rather than on the amplitude. The same observation

applies for low-stress tests of 2024-T3. However, the data from tests

of 2024-T3 at high stresses fell somewhat higher on the diagram than for

tests at $R = 0$. This would indicate some effect of amplitude in the

behavior of this material.

- 13 -

One possible explanation for the differences in behavior of the two materials may be suggested on the basis of the relative magnitude of yield stresses in the two materials and on considerations of crack closure during compression loading. The 2024-T3 material has a lower yield strength and is somewhat more ductile than 7075-T6. Thus it is reasonable to expect more plastic deformation at the tip of the crack in 2024-T3 than in 7075-T6 tested at the same stress. Photomicrographs of fatigue cracks in specimens of each of the materials are presented in figure 9. The cracks were approximately 1.8 inches long in each specimen and the test stress was 30 ksi in each case. Both pictures were taken when the specimen was unloaded. It is quite evident that the crack opens wider in 2024-T3 than in 7075-T6. From these observations it seems reasonable that the crack can close readily in 7075-T6 when the specimen is subjected to compression loading. The same action probably takes place in 2024-T3 specimens tested at low stresses which do not produce large plastic deformations. If the crack can close completely under compression loading, the crack does not act as a stress raiser in compression and the stress history at the crack tip will be essentially at $R = 0$ even when the applied load is at $R = -1$. However, if the crack cannot close readily, the material at the tip of the crack experiences high compression stresses and a higher rate of crack propagation is obtained in 2024-T3 specimens tested at $R = -1$ than in those tested at $R = 0$. The higher rate of crack propagation in specimens of 2024-T3 material tested at high stress can probably be attributed to such action.

Fatigue crack propagation tests conducted by Heywood at the RAE (ref. 24) on 36-inch-wide specimens of DTD 546B were also plotted in the

- 14 -

suggested coordinate system. These results are presented in figure 10. The value of ρ_e used to compute K_N was 0.002 inch, the same as that used for the Al-Zn-Mg alloy 7075-T6. The empirical curve shown is the same as that given in figure 7 for NASA tests at $R = 0$. The agreement is again seen to be quite good. It is interesting to note that one of Heywood's tests was conducted with the applied stress progressively decreased to keep S_{NET} a constant at 15 ksi. The results of this test also fall in line with the others.

It appears that the proposed procedure is based on rational considerations and has been shown to correlate the results of a test with a variety of widths and crack lengths.

In all the correlations just discussed, the maximum values of $K_N S_{NET}$ reach approximately 600 ksi. When applied to steels the values go even higher. Such high stresses are, of course, fictitious. Physically, it may be more appropriate to consider equivalent strain, but consideration of plastic deformations would be required and these complicate the calculations. Attempts at correlation by stress concentration factors in the plastic range are probably not advisable because practically all data would lie in the narrow range between the yield and ultimate tensile strengths of the material. A much less sensitive correlation would be achieved. At the low stress end of the $K_N S_{NET}$ scale, where the values are used to determine ρ_e from tests establishing the minimum stress required to propagate a crack, the values of $K_N S_{NET}$ are in the elastic range and probably are more nearly the actual stress present.

The use of the proposed method to predict crack length as a function of cycles of load requires the integration of the equation presented. This is quite cumbersome and can be done only by numerical methods. A simplification is possible by adopting Head's (ref. 4) equation

$$\frac{dl}{dN} \approx 2\alpha l^{3/2}$$

as an approximation. The value of α may be estimated from the equations proposed earlier by equating the expression

$$\frac{dl}{dN} = \log_{10}^{-1}\left(0.00509K_N S_{NET} - 5.472 - \frac{34}{K_N S_{NET} - 34}\right)$$

with that of Head to yield:

$$\alpha = \frac{1}{2} l^{-3/2}\log_{10}^{-1}\left(0.00509K_N S_{NET} - 5.472 - \frac{34}{K_N S_{NET} - 34}\right)$$

This value of α is reasonably constant, at least for short cracks, since the factor $l^{-3/2}$ partially counteracts the variation in $K_N S_{NET}$ with crack length. The integration yields

$$N = C - \frac{1}{\alpha} l^{-1/2}$$

where N is the number of cycles measured from some initial crack length and C is a constant of integration which may be determined by computation when $N = 0$. Crack propagation curves obtained in this manner produce a reasonable estimate of the curves plotted from test data.

For tests with other combinations of mean and alternating stresses it is reasonable to expect a family of curves in a diagram of rate of crack propagation plotted against $K_N S_{NET}$. The studies of Frost and Dugdale (ref. 8) provide data from a series of tests with a systematic variation in test stresses. The tests have been analyzed and plotted in figures 11 and 12 for mild steel and aluminum, respectively. The curves have been identified in terms of R values because this quantity remains constant throughout the test, whereas some other parameter, such as mean stress on the net section, varies continuously during the test. Curves in the figure were computed for constant values of the factor k proposed by Frost and Dugdale and only in the range where this factor is recommended (crack lengths less than 0.12 times the width of the specimen). The effective radius ρ_e was taken to be 0.003 inch for both materials. A consistent family of curves is obtained as expected. Generally speaking, the curves for successively higher values of R lie to the lower right of curves for lower values of R in the figure. The left end of each curve should become asymptotic to the minimum stress for propagation of cracks at that value of R and this appears to be a reasonable limit in each case. Additional work is required to establish the relation between the various curves presented.

Some discussion of the effective radii used in the foregoing correlations is in order. Obviously, radii of the order of 0.002 or 0.003 inch are far in excess of the actual radius of curvature at the crack tip. One reason is that the material at the tip of the crack has been subjected to very large plastic deformations and complex residual compressive stresses are undoubtedly present. These factors have not

been accounted for explicitly in the procedure outlined and probably cannot be without undue complication. These effects are reflected in the magnitude of the effective radius. Both the residual compression stress and the change in local curvature due to plastic deformations would contribute to a decrease in notch severity which would, in turn, result in a large value of ρ_e.

The influence of plasticity on rate of crack propagation can be quite important. A case in point is shown in figure 6 where the data for a test of a 2024-T3 specimen at 50 ksi fell substantially above the rest of the data. At this stress level, essentially the entire net section of the specimen is in the plastic range, and the possible beneficial effects of residual compressive stresses are eliminated. Consequently, the material ahead of the crack is more vulnerable to the sudden bursts of crack growth described earlier and the average rate of crack propagation is higher.

OTHER METHODS FOR COMPUTING RATES OF CRACK PROPAGATION

Frost and Dugdale (ref. 8) have proposed that the rate of crack propagation is given by $\frac{dl}{dN} = kl$ and have found good agreement with behavior of short cracks in 10-inch-wide specimens tested at low-stress levels. To be generally valid, the relation should also correlate results of tests of other sizes of specimens. The data of McEvily and Illg (ref. 13) afford an opportunity for an evaluation. These data for 7075-T6 aluminum alloy have been analyzed according to the Frost-Dugdale relation and the results are presented in figure 13 as a curve of

- 18 -

$\log \frac{dl}{dN}$ against $\log l$. The $K_N S_{NET}$ parameter proposed in this paper

has been used to extend the data in ranges for which no data were avail-
able. Data obeying the relation proposed by Frost and Dugdale should
appear as a straight line with a slope of one. The curves in figure 13
depart somewhat from straight lines of unit slope even within the range
of application proposed. In wide specimens the slope approaches one
only for low stresses. At high stresses the curves have slopes appreci-
ably higher than one, indicating that the rate of crack growth varies
with a higher power of the crack length. At low stresses and narrow
specimens, the $K_N S_{NET}$ expression predicts considerably lower crack
propagation rates than does the Frost-Dugdale relation. In this range
the crack lengths are less than 1/16 inch long and no reliable data are
available. A similar set of conclusions is obtained from analysis of
tests of 2024-T3 aluminum alloy and of 12 Mo V steel. Frost and Dugdale
limit the application of their relation to cases where the total crack
length is less than 12 percent of the width of the specimen, a restric-
tion which need not be applied to the $K_N S_{NET}$ relation.

Anderson and Paris (ref. 25) recently proposed that the rate of
crack propagation is determined by a stress intensity factor proportional
to $S\sqrt{l}$. This factor is very similar to the expression proposed in this
paper. In the expression

$$K_N S_{NET} = \left[1 + \frac{1}{2}\left(K_c - 1\right)\sqrt{\frac{l}{\rho_e}} \right] S_{NET}$$

the product $(K_c - 1)$ S_{NET} is essentially constant for crack lengths up to one-half the width of the specimen and, if the first term in the bracket is neglected, $K_N S_{NET}$ becomes proportional to $S_{NET}\sqrt{l}$. Thus, the Anderson-Paris relation is essentially equivalent to the relation previously developed and demonstrated in this paper. The two methods should produce approximately equivalent agreements with test data.

OTHER FACTORS AFFECTING CRACK PROPAGATION IN
SIMPLE SPECIMENS

Conditions at the tip of a crack can be affected by a variety of influences with resultant effects on crack growth. For example, two-step tests of 2024-T3 and 7075-T6 sheet specimens have demonstrated a significant delay in crack propagation when the second stress level was lower than the first. A typical result is shown in figure 14. Each of the three curves in the figure represents crack growth at 30 ksi after the crack reached a length of 0.4 inch by repeated stresses S_1 of 50 ksi, 30 ksi, or 6 ksi, respectively. If the crack propagation curve for the constant level test (30 ksi) is regarded as normal behavior, the crack growth was also normal when the stress was increased from 6 to 30 ksi. This result was general for the several cases tested. However, when the stress level was decreased from 50 ksi to 30 ksi, crack growth was delayed by some 10,000 cycles. Once started, the crack growth rate again became and remained normal for 30-ksi stress. The results of a series of such tests in which the stress level was reduced are summarized in figures 15 and 16 for 2024-T3 and 7075-T6 aluminum alloys, respectively.

The delay in propagation is plotted against the second stress level for various values of the first stress level. Quite naturally, the delay is longer for large changes in stress level and for high first stresses. The delays range up to 10^7 cycles and, in at least one test for each material, the crack refused to propagate at a level substantially higher (by about 10 ksi) than the minimum stress required to propagate cracks of equal length in constant level tests. This amounts to an increase in fatigue limit by a factor of more than two to one. The basic action is probably one of introducing a residual compressive stress which in turn reduces the local mean stress such that the local stress range remains below the minimum value required for crack propagation.

Christensen (refs. 26 and 27) and Haas (ref. 28) have conducted similar tests and found some increase in rate of crack propagation when the second stress level was higher than the first. However, this effect was quite small compared with the effects observed when the second stress level was lower than the first.

The delay in crack growth and the change in fatigue limit of the specimen are undoubtedly factors in any study of cumulative damage. The linear hypothesis of cumulative damage or simple modifications of it cannot predict the effects noted here. Fortunately, the only consistent effect noted tends to lengthen fatigue life, thus, predictions by the simple rules should be on the safe side.

The study of fractographs of fatigue specimens tested under more complicated load schedules provides additional information on the effects of stress changes. Tests were conducted on specimens machined from 3/4-inch-thick 2024-T4 bar stock to simulate aircraft spar caps. Loading

schedules of the kind shown in figure 17 were chosen which included a
selection of representative loadings. Stress cycles of 10 ± 3 ksi were
applied in large numbers to simulate a low-intensity gust loading and
single cycles of higher amplitudes of stress were applied from time to
time during the test. The important findings of this investigation may
be described by reference to only the first few cycles of high load in
each of the two tests indicated in the figure. In schedule A the first
of the single load cycles had an amplitude of ± 6 ksi, the second ± 8,
the third ± 6, the fourth ± 4, and then the sequence of 8-, 6-, and 4-ksi
cycles was repeated. In each case approximately 2,000 cycles at ± 3 ksi
were applied between the single cycles of higher stress. In the
schedule B the sequence is the same with the exception that each sequence
of high loads started with a cycle at ± 10 ksi and progressed through ± 8,
± 6, ± 4, ± 10, ± 8, and so forth. Again, approximately 2,000 cycles of
10 ± 3 ksi stress were applied between the single cycles of higher stress.
Photographs of the fracture surfaces of these two specimens are presented
in figure 18. These fracture surfaces exhibit the familiar pattern of
alternately dark and light bands that is characteristic particularly of
specimens tested with programmed loadings. In specimen A the first
single cycle of ± 6 ksi produced a small, but clearly visible dark band,
the first cycle at ± 8 ksi, and all subsequent cycles at ± 8 ksi produced
more prominent dark bands but all later applications of ± 6 ksi did not
produce visible markings. In specimen B the dark bands seen in the
fractograph are the result of single cycles at ± 10 ksi and the ± 8-ksi
cycles did not produce visible markings. In each case it seems reasonably
certain that the interspersed 2,000 cycles of low stress produced some

crack propagation. The most plausible explanation for these observations is that residual stresses produced during the highest load cycles of a test had a strong delaying influence on crack propagation at subsequent lower stresses which would otherwise have contributed a measurable burst of crack growth. Some effect of residual stress must be present even after some fatigue cracking at lower stresses.

Obviously, more work is required to explore this phenomenon further. It seems reasonable to expect that the influence noted would disappear if larger numbers of low stresses had been employed. For the present, however, the prospects for reconstructing a service experience from inspection of a failed part are not encouraging.

In the foregoing discussions strong emphasis has been placed on local stresses as controlling factors in crack propagation. A reasonable next question concerns the possible effect of variations in metallurgical characteristics of the material on rate of crack propagation. An unpublished exploratory study has been performed on two Al-Zn-Mg alloys which differed mainly in the iron and silicon content. One material was the conventional 7075-T6 aluminum alloy and the other a special alloy designated X7275-T6 which had lower iron and silicon and a correspondingly lower number and smaller size of constituent particles. These microstructures are shown in figure 19 and the mechanical properties of each of the materials, are listed in table I. Fatigue crack propagation tests were conducted in axial load at $R = 0$ on 2-inch-wide sheet specimens. Figure 20 presents the resulting crack propagation curves, obtained by averaging four crack lengths obtained in two tests of each material. The stress level in each test was 13 ksi. The curves indicate

that the number of cycles required to produce an increment of crack growth in 7075-T6 aluminum alloy was almost twice that required to produce the same increment of growth in the "cleaner" X7275-T6. Although the data available are limited, the scatter is small and the effects are considered significant. Hempel (ref. 29) showed by photomicrographs that cracks tended to grow through the particles in aluminum-alloy specimens. This suggests that the particles may act as temporary "crack-stoppers." No significant crack-stoppers were present in the X7275-T6; therefore, a higher rate of crack propagation resulted. Whether or not 7075-T6 aluminum alloy may be benefitted by adding additional constituent particles is problematical since it is well known that materials with high inclusion content tend to have low ductility and a corresponding reduction in notch strength.

Another manipulation of metallurgical factors to improve some material property is that of intentionally decarburizing high-strength steels to improve their notch strength. The effects of this procedure on fatigue crack propagation and notch strength of a 12 Mo V steel have been studied. The mechanical properties listed in table II show that the decarburization produced a reduction in tensile strength but improved the notched strength of this material. Figure 21 presents the results of fatigue crack propagation tests on both decarburized and normal material. The data are plotted against the parameter $K_N S_{NET}$ computed with $\rho_e = 0.0015$ inch for both the decarburized and normal materials. This value was chosen to produce best overall correlation of the data from tests evaluating the residual static strength of specimens containing internal cracks. The data lie in a narrow scatter band in the

figure indicating that the rates of crack propagation were very nearly
the same in the two materials. Evidently the rate of crack growth is
governed chiefly by the conditions in the interior of the specimen.
This contrasts with the surface factors which are recognized as having
a very important effect on crack initiation.

NONPROPAGATING CRACKS

During the past several years a number of studies have been con-
ducted by several investigators to explain nonpropagating cracks. These
studies and the explanations offered indicate that nonpropagating cracks
occur for at least four different reasons. Although many of these cracks
appear to be academic curiosities rather than of real engineering signifi-
cance, they will be discussed here for the sake of completeness in pres-
entation and to show that three of the types can be explained with the
aid of local stress considerations utilized in this paper. In each type
of crack to be discussed it is assumed that the stress amplitude is
maintained constant at some low level. Obviously, any of these cracks
will grow if the applied stress is high enough. In service, the cir-
cumstances required for nonpropagating cracks are encountered only very
rarely.

One type of nonpropagating crack has been discussed in a previous
section on effects of variable-amplitude loading. Cracks were found
which did not propagate after the stress was changed from a high to a
low level. The local stresses which are probably operative are illustrated
in diagram a of figure 22. The residual stress at the tip of the crack
is compressive as shown for the initial part of the curve. Subsequent

application of a low stress increases the local stress, as shown in the second part of the curve, but the maximum stress is below the fatigue limit. Thus, no propagation occurs even though the amplitude of local stress might have been high enough to propagate the crack in the absence of the residual stress. This type of nonpropagating crack plays an important role in the study of cumulative damage where it must probably be considered when improved methods are developed for estimating life under variable-amplitude loads.

A second type of nonpropagating crack, discussed by McEvily and Illg (ref. 13) sometimes occurs at a notch which has a smaller radius than the effective radius ρ_e for cracks in the material. The action is shown in diagram b of figure 22. The value of $K_N S_{NET}$ for the notch is assumed to be slightly higher than the fatigue limit of the material as indicated by the initial portion of the curve. As soon as the crack has formed the effective radius is greater than for the notch, the stress decreases below the fatigue limit as shown, and crack growth stops. Many of the cracks studied by Frost can be explained in this way.

A third kind of nonpropagating crack, represented in part c of figure 22 can be produced in tests with completely reversed stress cycles if the crack has an opportunity to close under compression loads. This type has been discussed by Coffin (ref. 30) and McEvily and Illg (ref. 13). In this case the value of $K_N S_{NET}$ for the initial notch is just above the fatigue limit for completely reversed stress, so the crack is formed. If ρ_e is less than the radius of the notch, the local stress $K_N S_{NET}$ is increased somewhat, as shown in the figure. However, the closure of

the crack reduces the effect of the compression part of the cycle so
that the fatigue limit for $R = 0$ becomes the critical stress which
must be exceeded. Cracks of this type will be produced in a very limited
range of combinations of combined stress and notch configurations.

Wadsworth (ref. 14) has found a fourth kind of nonpropagating cracks
which occur for metallurgical reasons. These cracks were initiated in
0.5 percent C steel at pearlite-ferrite interfaces because of local stress
concentrations, but these cracks could not propagate because the overall
stress level was not sufficient for cracks to grow through the ferrite
matrix.

Frost (ref. 31) proposed a relation

$$S^3 l = \text{Constant}$$

(where S is the amplitude of stress on the gross cross section) to
govern the minimum stress required for crack propagation. He demonstrated
good correlation with a variety of tests of specimens ranging from rotating
beams with circumferential grooves to 10-inch-wide sheet specimens with
central slits tested under axial loads. Most of the data were from
tests with completely reversed loading, but a few were from tests with
a mean tension load. The effect of the mean load was found to be small
and was neglected in the analysis. The good agreement between test data
and predictions by this empirical expression is remarkable in view of
the variety of test and specimen conditions involved. However, the
presence of the factor S^3 in the expression bears scrutiny for a
physical explanation.

It is of interest to test the present method against the data correlated by Frost with his expression. The curves in figure 23 present a comparison between Frost's curve and a curve predicted by the expression

$$S = \frac{S_f}{1 + \frac{1}{2}(K_c - 1)\sqrt{\frac{l}{\rho_e}}}$$

in which the stress concentration factors were computed for 10-inch-wide specimens with central slits. The $\rho' = \rho_e$ value used was 0.016 inch to produce good agreement with the test data. This value of ρ_e is higher than the value 0.003 inch used by McEvily and Illg (ref. 13) to correlate a more limited sample of Frost's data on tests of mild steel. It is felt that the larger value of ρ_e needed here is brought about by various changes of stress level in the Frost tests. In some cases the same specimen was tested at progressively higher stress levels which are known to produce "coaxing" effects in mild steels. The prediction by the present method is seen to be in good agreement with the Frost curve, but of course, this agreement should apply for the 10-inch-wide specimens only.

A comparison between the present procedure and Frost's results for all the configurations treated is shown on figure 24. For this comparison the stress concentration factor K_N for each configuration was computed and multiplied by the nominal stress S_{NET} applied to the specimen. These products were plotted against the crack length present in each

- 28 -

specimen. In this case, $\rho' = \rho_e = 0.012$ inch was used in the calculations. The $K_N S_{NET}$ values are seen to lie in a reasonably narrow horizontal band which has a mean value approximately equal to the fatigue limit for unnotched specimens of this material. The present method appears to correlate the same data in a satisfactory way. ~~Its application can again be expected to be more general because its applicability is not limited to short cracks to which limit Frost's relation must be limited.~~

CRACK PROPAGATION IN BUILT-UP STRUCTURES

The foregoing discussion has been limited to phenomena which occur in simple specimens for which stress distributions may be estimated with good reliability with reasonably simple mathematical treatments. In practice, however, designers and operators are concerned with very much more complex structural configurations. Some testing has been done on such configurations by NASA and some of the more consistent lessons learned from them will be reviewed.

In one of these investigations Hardrath and Leybold (ref. 33) conducted repeated bending tests of beams such as the one shown in figure 25. Overall dimensions of beams were 20-inch chord, 6-inch depth, and 8-foot length. The covers were 0.051 inch thick and had 8 stringers attached. The stringers were either riveted or bonded to the sheet or machined integrally with the skin. Beams were constructed of 2024-T3 and of 7075-T6 aluminum alloys. The tension covers were cambered slightly to compensate for shear lag effects and thus produce essentially uniform stress across the middle of a center section of a carry-through bay.

- 29 -

The beams were supported at the ends and loads were applied at two span-wise stations, one at each end of the carry-through bay. Cracks started at a small slit in the center of the skin. The cross section of the riveted and bonded covers was the same and all covers had the same total area. The test stress in the tension cover was 13 ± 6.5 ksi.

The crack propagation curves obtained in these tests are presented in figures 25 and 26 for 2024-T3 and 7075-T6 beams, respectively. The percent of the total tension cross section lost by cracking is plotted against the number of cycles of load applied after the crack was first detected. A 20-inch-wide simple sheet specimen of the same material was tested under repeated axial loads at the same stress level for comparison. The curves indicate approximately equal and very rapid growth in the integrally stiffened and simple sheet specimens. Thus, the integral stiffeners were not effective in controlling crack growth. Cracks grew less rapidly in the box with the stringers riveted to the skin, principally because the cracks grew into rivet holes and hesitated there until new cracks were initiated on the opposite sides of the rivet holes. Crack growth became quite rapid after stringers started to fail. In spite of the fact that the bonded construction had no rivet holes to act as "crack-stoppers" the stringers must have controlled the skin stresses effectively enough to slow down the crack growth. In this construction no stringers failed before the crack had progressed completely through the skin; thus the crack growth, measured in terms of area lost, was slower than in either of the other two constructions.

Thus far, no adequate analytical procedure has been developed to predict all these results. It appears, however, that the simple method

proposed in the present paper might be adequate for treating the integrally stiffened construction. The change of stress concentration for a crack in a sheet with a single stringer located centrally across the crack has been treated analytically by Sanders (ref. 34). These procedures and others like them should help to produce analytical methods for estimating rates of crack growth in structures.

The influence of rivet pitch on rate of crack propagation was studied in additional tests (ref. 35) of other beams in which rivet pitch was the only parameter changed. The results of these tests on beams constructed of 7075-T6 aluminum alloy are presented in figure 27. The rates of crack growth are progressively higher for progressively greater rivet pitch. This result might be expected intuitively because a stinger must be more effective in restraining extensions of the sheet when the rivet pitch is small, but must be essentially without effect on local stress when the rivet pitch is large. No analytical studies appear to have been developed for the distribution of stresses in a cracked sheet as a function of rivet pitch. However, the studies of Budiansky and Wu (ref. 36) would indicate that such solutions might be forthcoming.

The effect of relative sizes of skin and stringers was studied in tension tests of stiffened panels by Whaley and Kurzhals (ref. 37). These results are presented in figure 28 in a plot similar to figures 25-27. These specimens were 30 inches wide with two heavy angles at the outside edges and four intermediate stringers. The proportion of the total area which was placed in the skin is shown on each curve. The remainder of the cross section was distributed among the stiffeners with one-eighth to each intermediate stringer and one-fourth to each

edge stringer. Cracks were again initiated at a slit in the center of the skin. All panels were tested at 14 ± 4.7 ksi. It is quite clear that panels with small stiffeners (high percentages of area in the sheet) experienced the highest rate of crack propagation and panels with progressively heavier stiffeners had correspondingly lower rates of crack growth. These results again agree qualitatively with Sanders' analysis (ref. 34) which indicates a greater reduction in stress concentration factor for heavier stiffeners. The temporary halting of crack growth when cracks grew into rivet holes is in evidence here in the same way as in the box beams. The very steep crack growth curve at the end of each test is due to failure of stiffeners.

An extensive series of fatigue tests of C-46 airplane wings by NACA provides additional information of interest here. These tests (ref. 38 through 42) included constant- and variable-amplitude loading schedules. In each case, the crack which ultimately grew through the entire tension surface was located in one of the two cross sections shown in figure 29. The cross section at wing station 214 contained two inspection cutouts and the assortment of stiffening members shown. Both cutouts were potential sources of crack initiation. Critical cracks also grew from joggles in doubler plates at wing station 195 just outboard of the wing joint. This cross section contained no cutouts. The chordwise distribution of stress in the wing indicated a maximum just aft of the spar. It is of interest to note that the crack propagation curves for each of these three failure locations had characteristic shapes such as those shown in the figure. Cracks starting at the cutout labelled I usually grew aft, but were considerably delayed by the heavy spar cap

and the heavy T-stiffener just forward of the cutout. This first increment of growth included failure of the half-T stiffener aft of the cutout for a total of some 5 percent of the tension area. When crack propagation resumed, it was in either of the large stiffeners and very rapid growth followed failure of one or both of these members. This behavior was most common in constant-level tests.

In a few cases the crack started in location II and grew aft with apparently little effect due to the hat stiffeners in its path. Although very long cracks were produced, area was lost slowly. However, when all material between the spars had failed, the front spar was somewhat overloaded and cracks grew in it. When this member failed, complete collapse was imminent.

In almost all variable-amplitude tests the cracks started at the joggle in the doubler (location III). This crack grew steadily through both doublers and the skin. The heavy spar cap failed in only one case before the test was stopped. This spar seems to have had sufficient strength to resist cracking and tended to slow down the rate of crack growth in the vicinity. In one test a sharp notch was cut in this member to force failure in it, but the crack refused to grow.

In agreement with the results of the tests of tension panels the tests of C-46 wings indicate that heavy stiffening members can limit both the extent and the rate of crack growth. As of this writing the available stress analysis methods are not adequate to estimate the results quantitatively. However, these results and those obtained elsewhere should help to build a fund of information which will guide

experienced designers to anticipate qualitatively the behavior to be expected from competing designs.

CONCLUDING REMARKS

The propagation of fatigue cracks in a variety of tests of sheet specimens and built-up structures has been reviewed.

An engineering method of estimating the rates of crack propagation has been described. This method is based on considerations of stresses at the crack tip. The method produced good correlation of results from tests of specimens varying in width between 2 inches and 36 inches and containing cracks up to one-half the width of the specimens. The range of conditions for which the method appears applicable is considerably greater than that of other methods.

The following additional conclusions may be drawn from tests of simple specimens:

1. The rate of crack propagation was found not to be sensitive to the compression parts of load cycles when the crack had an opportunity to close, but was sensitive to compression stresses when cracks did not close.

2. A change in stress level from a high to a low level produced a considerable delay in crack propagation. This delay increased with the magnitude of the initial stress and with the increment between stress levels. No important effects on rate of crack propagation were noted in tests in which the stress level was changed upward.

3. In tests of two aluminum alloys with closely similar chemical compositions but somewhat different dispersion of constituent particles

the rate of crack propagation was lower in the material having the larger number of particles.

4. Crack propagation rates were not affected by decarburization of the surface of specimens made of 12 Mo V steel.

5. Nonpropagating cracks have been discussed and four possible methods of producing them discussed. Three of these types may be explained with the aid of local stress considerations developed herein.

The rate of crack propagation in built-up structures depended heavily on the relative weights of skin and stringers, their mode of connection to each other, and the general configuration. Although the available stress analysis procedures do not permit a quantitative correlation of these results, the results are in qualitative agreement with each other when considered in light of the stresses operating in the vicinity of the crack. These observations and others like them should contribute to the fund of experience which will aid designers to provide structures resistant to crack propagation.

REFERENCES

1. Crussard, C., Plateau, J., Tamhankar, R., Henry, G., and Lajeunesse, D.:
   A Comparison of Ductile and Fatigue Fractures, Fracture.   John
   Wiley & Sons, Inc., New York, 1959, pp. 524-561.

2. Holden, J.:   The Formation of Sub-Grain Structure by Alternating
   Plastic Strain.   Phil. Mag., vol. 6, no. 64, Apr. 1961, pp. 547-558.

3. McEvily, A. J., Jr., and Illg, W.:   A Method for Predicting the Rate
   of Fatigue-Crack Propagation.   Symposium on Fatigue of Aircraft
   Structures, A.S.T.M., STP 274, 1959, pp. 112-119.

4. Head, A. K.:   The Growth of Fatigue Cracks.   Phil. Mag., vol. 44,
   July-Dec. 1953, pp. 925-938.

5. Orowan, E.:   Theory of the Fatigue of Metals.   Roy. Soc. London Proc.,
   ser. A, vol. 171, no. 944, May 1, 1939, pp. 79-106.

6. Forsyth, P. J. E., and Ryder, D. A.:   Some Results of the Examination
   of Aluminium Alloy Specimen Fracture Surfaces.   Metallurgia, vol. 63,
   no. 377, Mar. 1961, pp. 117-124.

7. Cottrell, A. H.:   Theory of Brittle Fracture in Steel and Similar
   Metals.   Transactions of the Metallurgical Society of AIME, vol. 212,
   1958, pp. 192-203.

8. Frost, N. E., and Dugdale, D. S.:   The Propagation of Fatigue Cracks
   in Sheet Specimens.   Jour. Mech. and Phys. of Solids, vol. 6,
   1957-1958, p. 92.

9. Frost, N. E.:   Propagation of Fatigue Cracks in Various Sheet
   Materials.   Jour. Mech. Eng. Sci., vol. 1, no. 2, Sept. 1959,
   pp. 151-170.

10. Martin, D. E., and Sinclair, G. M.: Crack Propagation Under Repeated

    Loading. Proc. Third Nat. Congress Appl. Mech., 1959, pp. 595-604.

11. Lipsitt, H. A., Forbes, F. W., and Baird, R. B.: Crack Propagation

    in Cold-Rolled Aluminum Sheet. Proc. A.S.T.M., vol. 59, 1959,

    pp. 734-747.

12. McEvily, A. J., Jr., and Illg, W.: Comments on Paper by H. A. Lipsitt,

    F. W. Forbes, and R. B. Baird: Crack Propagation in Cold-Rolled

    Aluminum Sheet. Proc. A.S.T.M., vol. 59, 1959, p. 752.

13. McEvily, A. J., Jr., and Illg, W.: An Investigation of Nonpropagating

    Fatigue Cracks. NASA TN D-208, 1959.

14. Wadsworth, N. J.: The Influence of Atmospheric Corrosion on the

    Fatigue Limit of Iron-0.5 Percent Carbon. Phil. Mag., vol. 6,

    no. 63, Mar. 1961, p. 397.

15. Howland, R. C. J.: On the Stresses in the Neighborhood of a Circular

    Hole in a Strip Under Tension. Roy. Soc. of London Phil. Trans.,

    ser. A, vol. 229, no. 671, Jan. 6, 1930, pp. 49-86.

16. Sjostrom, Sverker: On the Stresses at the Edge of an Eccentrically

    Located Circular Hole in a Strip Under Tension. Aero. Res. Inst.

    of Sweden, no. 36, 1950.

17. Neuber, H.: Theory of Notch Stresses: Principles for Exact Stress

    Calculation. J. W. Edwards, Ann Arbor, Mich., 1946.

18. Kuhn, Paul, and Hardrath, Herbert F.: An Engineering Method for

    Estimating Notch-Size Effect in Fatigue Tests on Steel. NACA

    TN 2805, 1952.

19. Landers, Charles B., and Hardrath, Herbert F.: Results of Axial-Load Fatigue Tests on Electropolished 2024-T3 and 7075-T6 Aluminum-Alloy-Sheet Specimens With Central Holes. NACA TN 3631, 1956.

20. McEvily, A. J., Jr., Illg, W., and Hardrath, H. F.: Static Strength of Aluminum-Alloy Specimens Containing Fatigue Cracks. NACA TN 3816, 1956.

21. McEvily, A. J., Jr., and Illg, W.: The Rate of Fatigue-Crack Propagation in Two Aluminum Alloys. NACA TN 4394, 1958.

22. Grover, H. J., Hyler, W. S., Kuhn, Paul, Landers, Charles B., and Howell, F. M.: Axial-Load Fatigue Properties of 24S-T and 75S-T Aluminum Alloy as Determined in Several Laboratories. NACA TR 1190, 1954.

23. Illg, W., and McEvily, A. J., Jr.: The Rate of Fatigue-Crack Propagation for Two Aluminum Alloys Under Completely Reversed Loading. NASA TN D-52, 1959.

24. Heywood, R. B., and Norris, G. M.: Crack Propagation and Fatigue Strength of Some Aluminium Alloy Panels. R.A.E. Tech. Note No.: Structures 223, Mar. 1957.

25. Anderson, W. E., and Paris, P.: Evaluation of Aircraft Material by Fracture. Metals Eng. Quar. (ASM), vol. 1, 1961, p. 33.

26. Christensen, R. H.: Fatigue Cracking, Fatigue Damage and Their Detection. Metal Fatigue, McGraw-Hill Book Co., Inc., 1959.

27. Christensen, R. H.: Crack Strength and Crack Propagation Characteristics of High Strength Metals. First Quar. Prog. Rep. (Contract AF 33(616)-7444), Douglas Aircraft Co., Inc., 1960., pp. 4, 7.

28. Tibor, Haas: Reprint from Materials Testing. Vol. 2, 1960, no. 1 (pp. 1-17), p. 11.

29. Hempel, M. R.: Slip Bands, Twins and Precipitation Processes in Fatigue Stressing, Fracture. Technology Press, John Wiley & Sons, Inc., New York, 1959.

30. Coffin, L. F., Jr.: A Mechanism for Non-Propagating Fatigue Cracks. Proc. A.S.T.M., vol. 58, 1958, pp. 570-575.

31. Frost, N. E.: A Relation Between the Critical Alternating Propagation Stress and Crack Length for Mild Steel. Proc. Inst. Mech. Eng., vol. 173, no. 35, 1959.

32. Levy, J. C.: Comments on Paper by N. E. Frost: A Relation Between the Critical Alternating Propagation Stress and Crack Length for Mild Steel. Proc. Inst. Mech. Eng., vol. 173, no. 35, 1959.

33. Hardrath, Herbert F., Leybold, Herbert A., Landers, Charles B., and Hauschild, Louis W.: Fatigue-Crack Propagation in Aluminum-Alloy Box Beams. NACA TN 3856, 1956.

34. Sanders, J. Lyell, Jr.: Effect of a Stringer on the Stress Concentration Due to a Crack in a Thin Sheet. NASA TR R-13, 1959.

35. Hardrath, Herbert F., and Leybold, Herbert A.: Further Investigation of Fatigue-Crack Propagation in Aluminum-Alloy Box Beams. NACA TN 4246, 1958.

36. Budiansky, Bernard, and Te Wu, Tai: Transfer of Load to a Sheet From a Rivet-Attached Stiffener. Presented at 10th Internat. Congress Appl. Mech. (Stresa, Italy, Aug. 31 - Sept. 7, 1960), Harvard Univ., Feb. 1961.

37. Whaley, Richard E., and Kurzhals, Peter R.: Fatigue-Crack Propagation in Aluminum-Alloy Tension Panels. NASA TN D-543, 1960.

38. McGuigan, M. J., Jr., Bryan, D. F., and Whaley, R. E.: Fatigue Investigation of Full-Scale Transport-Airplane Wings. Summary of Constant-Amplitude Tests Through 1953. NACA TN 3190, 1954.

39. Whaley, Richard E., McGuigan, M. J., Jr., and Bryan, D. F.: Fatigue-Crack-Propagation and Residual-Static-Strength Results on Full-Scale Transport-Airplane Wings. NACA TN 3847, 1956.

40. Whaley, Richard E.: Fatigue Investigation of Full-Scale Transport-Airplane Wings. Variable-Amplitude Tests With a Gust-Loads Spectrum. NACA TN 4132, 1957.

41. Foster, Lee R., Jr., and Whaley, Richard E.: Fatigue Investigation of Full-Scale Transport-Airplane Wings. Tests With Constant-Amplitude and Variable-Amplitude Loading Schedules. NASA TN D-547, 1960.

42. Huston, W. B.: Comparison of Constant-Level and Randomized-Step Tests of Full-Scale Structures as Indicators of Fatigue-Critical Components. Proc. Symposium on Full-Scale Fatigue Testing of Aircraft Structures, Pergamon Press, 1961.

DULL APPEARANCE, STATIC FAILURE

BRIGHT APPEARANCE, MANY CYCLES OF LOAD

DIRECTION OF GROWTH
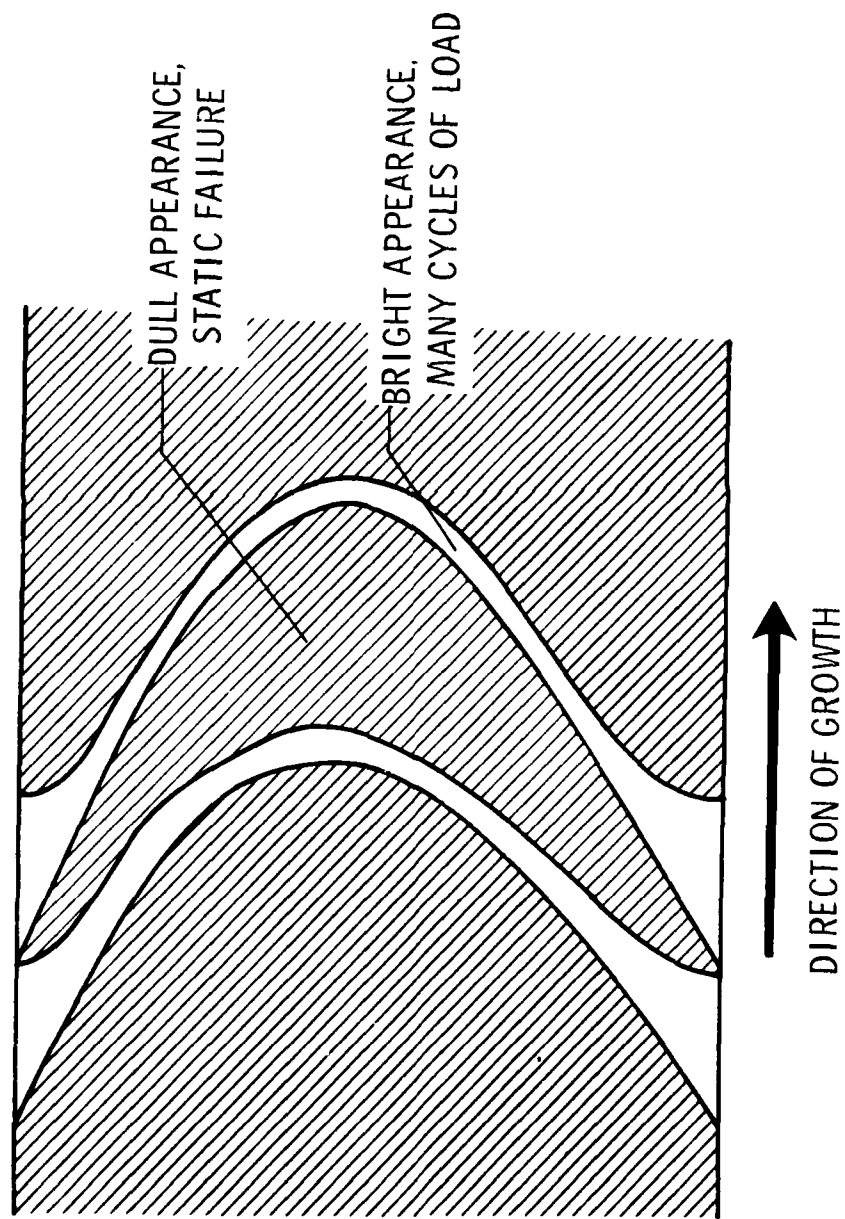
Figure 1.- Steps in growth of fatigue cracks in sheet.
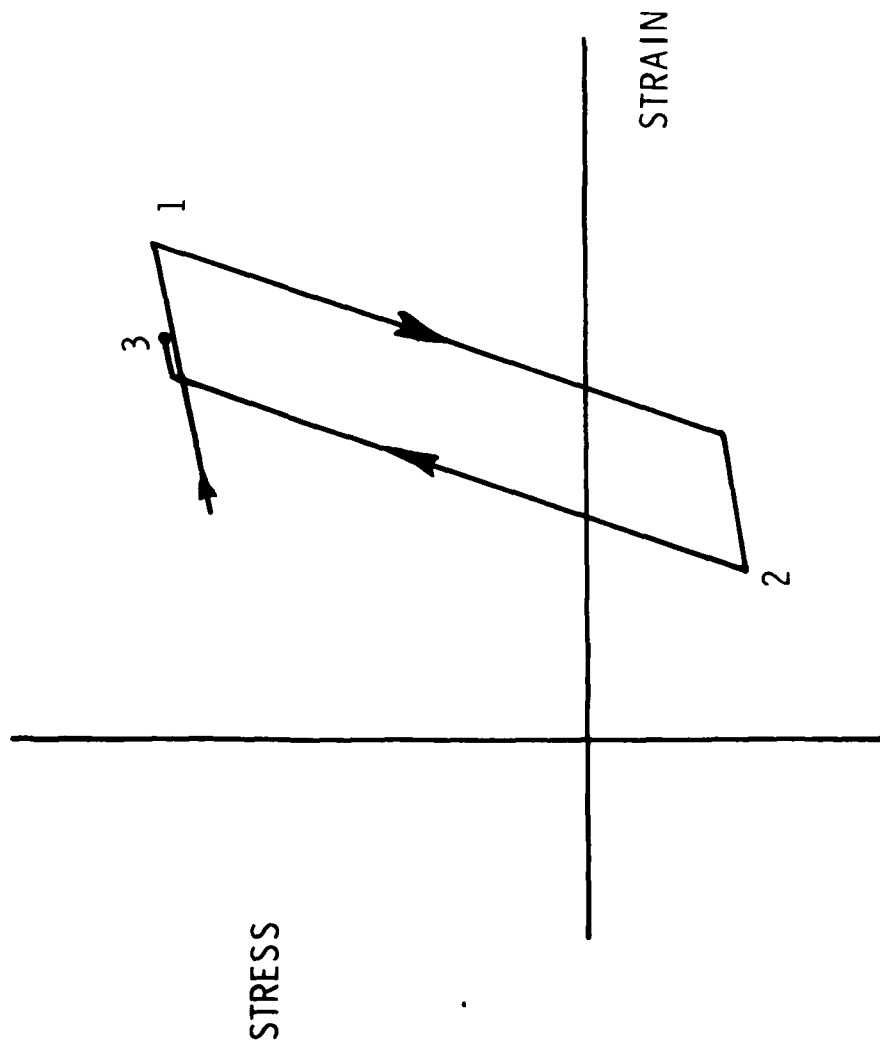
Figure 2.- Stress-strain relation at tip of a growing crack.
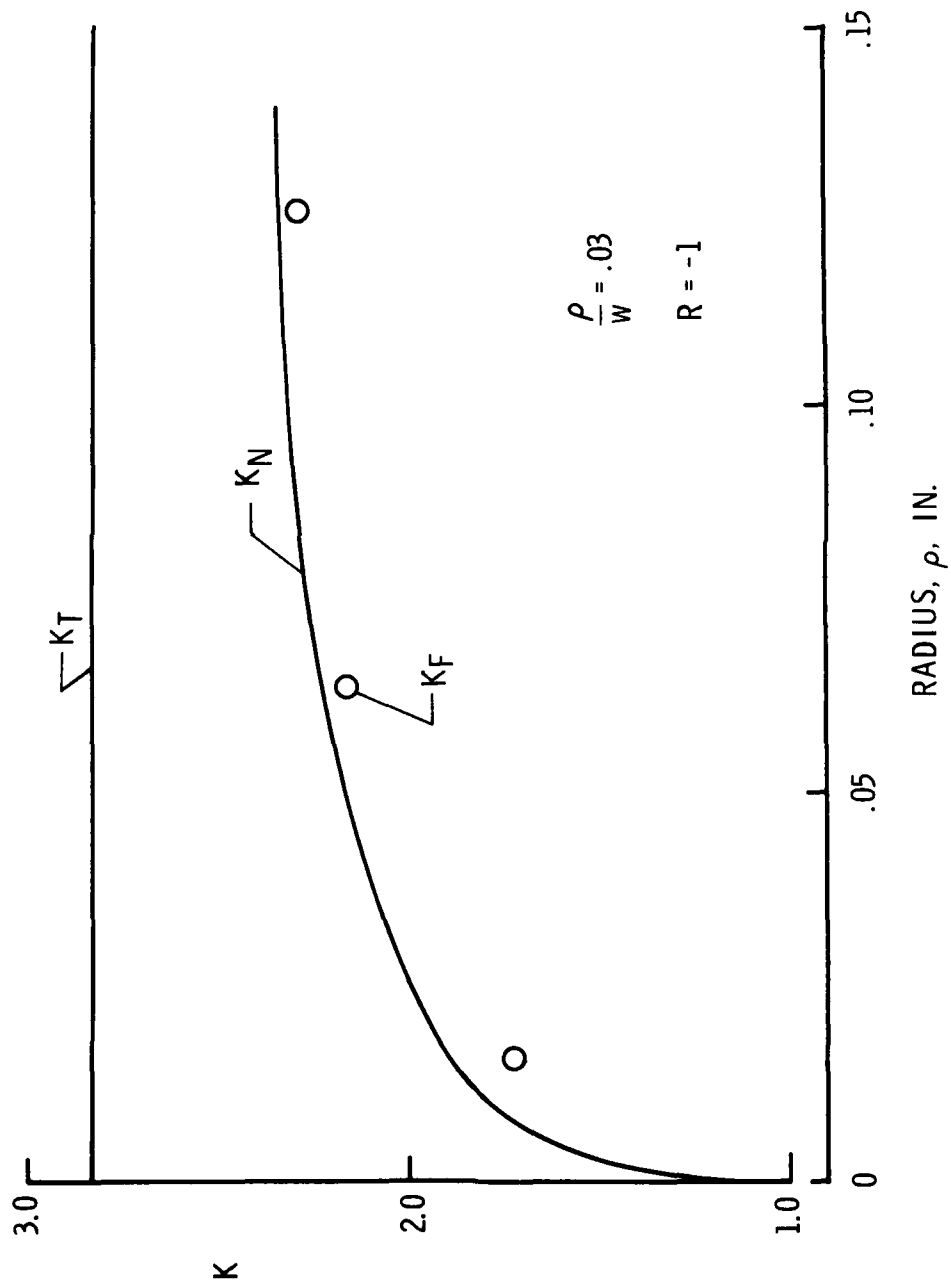
7075-T6 aluminum-alloy sheet with central holes.

$\dfrac{\rho}{w} = .03$

$R = -1$

RADIUS, ρ, IN.

Figure 3.- Fatigue notch size effect.
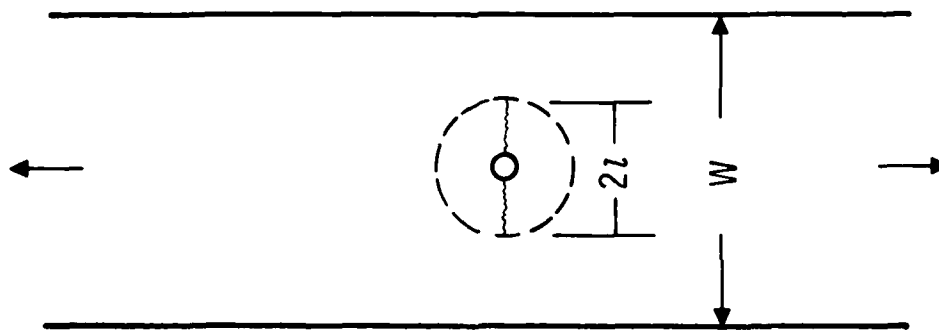
NASA

$$K_c \text{ FOR HOLE IN SHEET FROM HOWLAND}$$

$$K_e = 1 + (K_c - 1)\sqrt{l/\rho_e}$$

$$K_N = 1 + \frac{K_e - 1}{1 + \sqrt{\rho'/\rho_e}}$$

$$\text{FOR} \quad \rho' = \rho_e$$

$$K_N = 1 + \frac{1}{2}(K_c - 1)\sqrt{l/\rho_e}$$

Figure 4.- Computation of stress concentration factor for cracks.
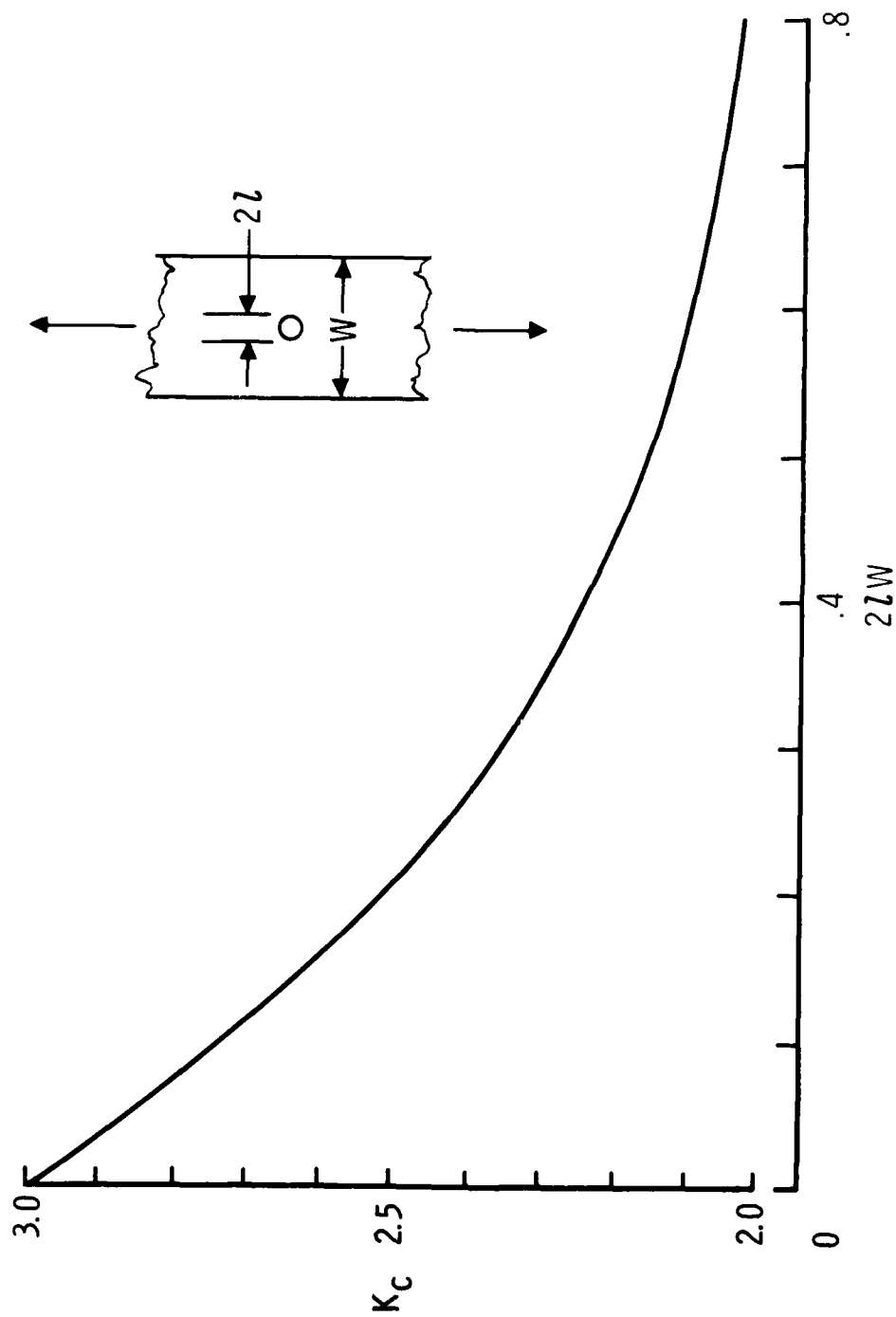
Figure 5.- Stress concentration factor for a circular hole in a finite sheet (Howland).
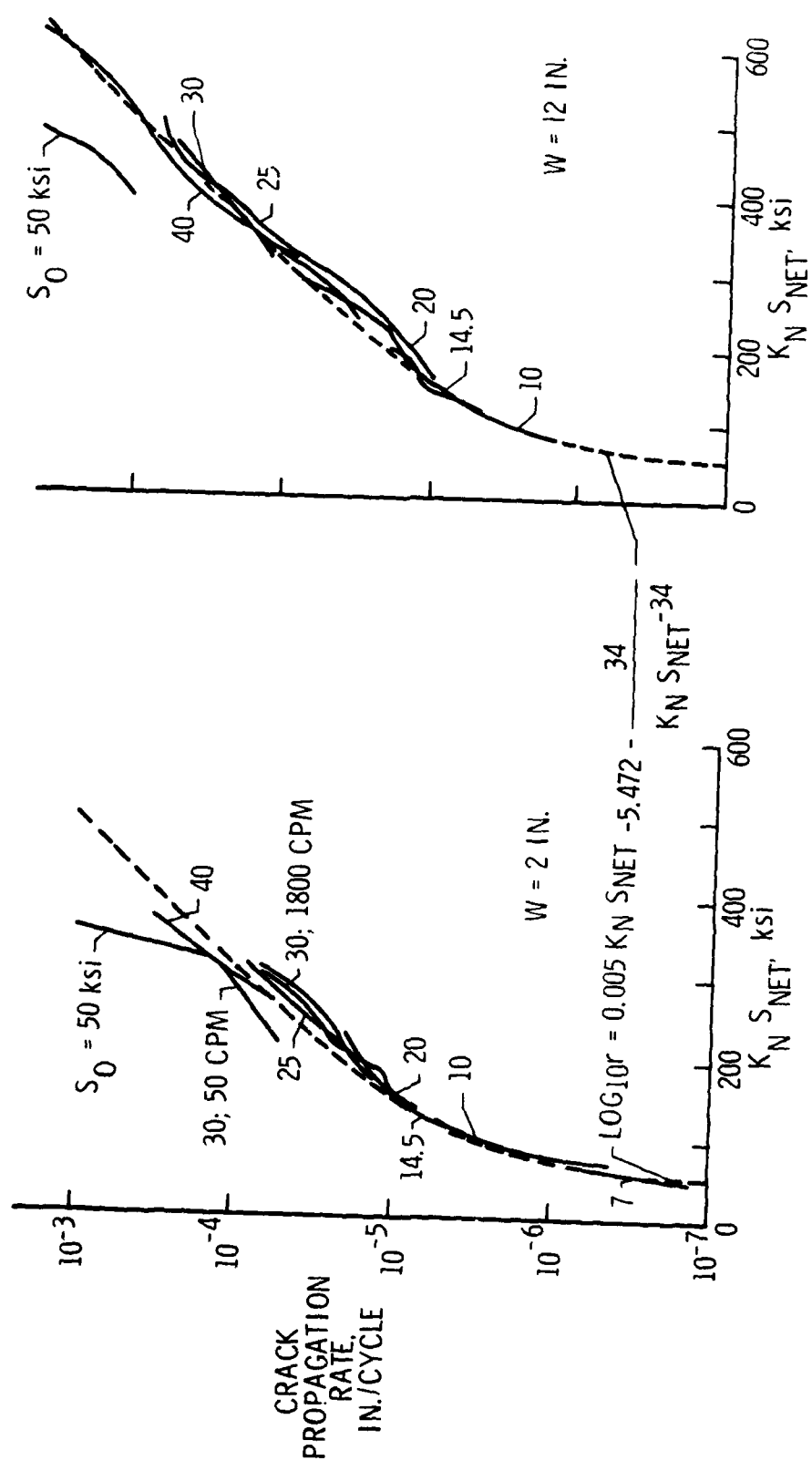
NASA

2024-T3 aluminum-alloy sheet, $R = 0$.

Figure 6.- Fatigue crack propagation.
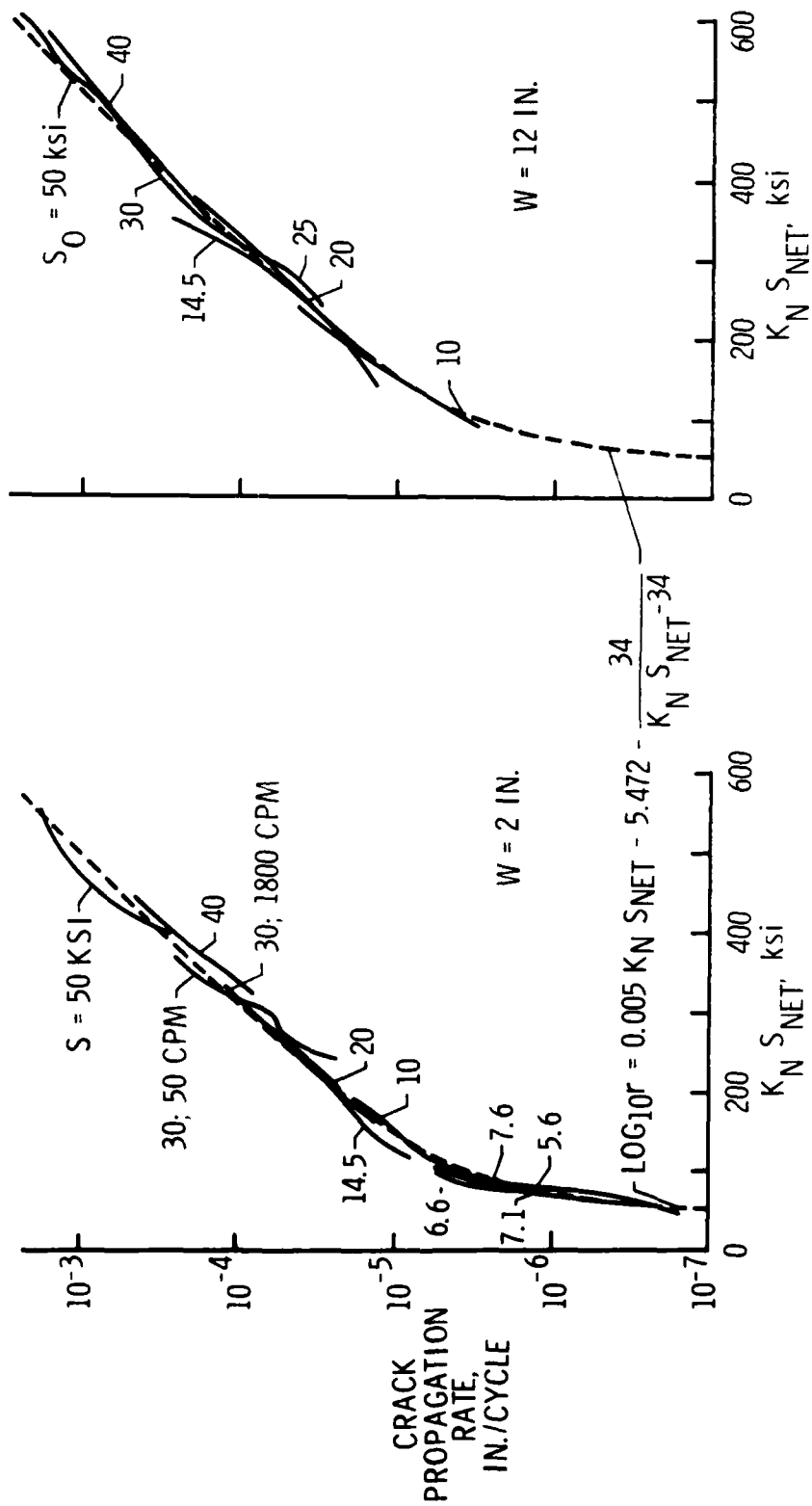
Figure 7.- Fatigue crack propagation.

7075-T6 aluminum alloy, R = 0.
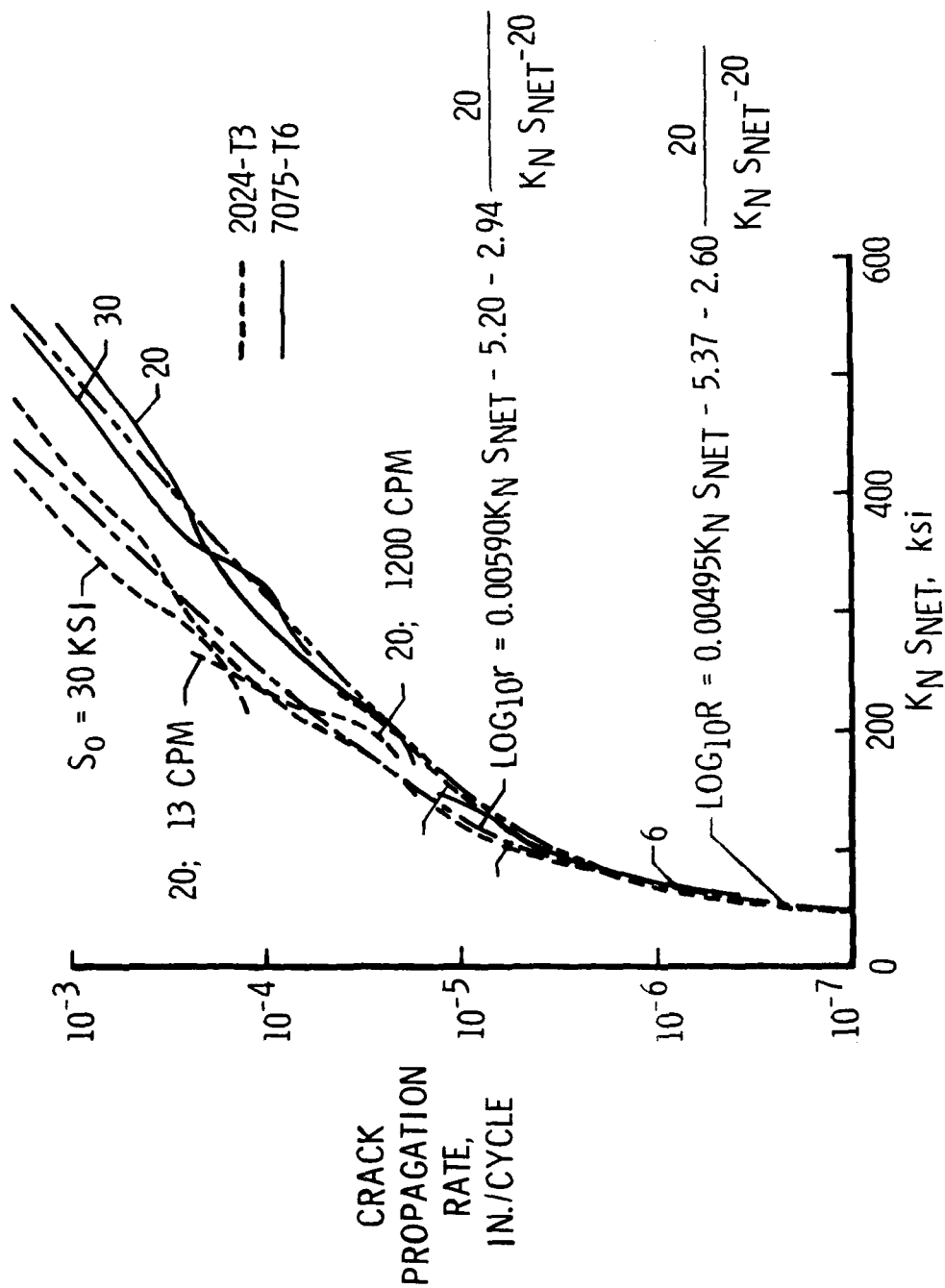
NASA

Two aluminum alloys, $R = -1$.

Figure 8.- Fatigue crack propagation.

.1 IN.
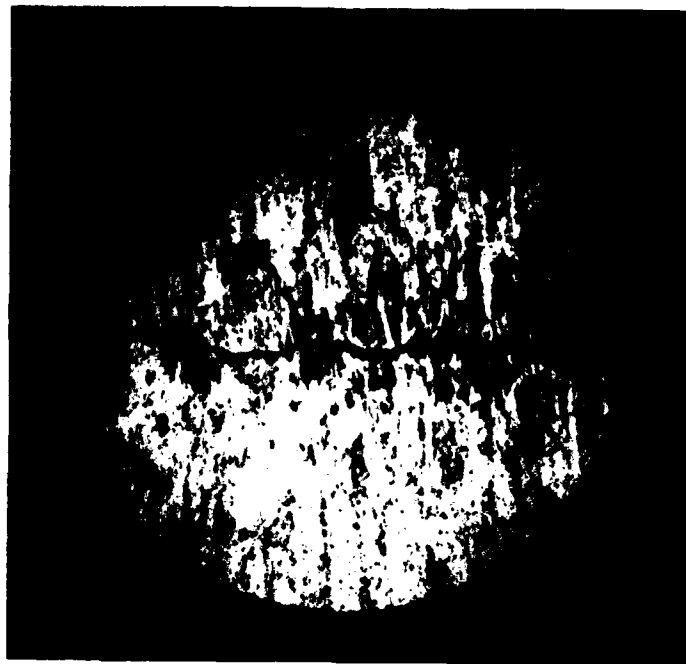
2024-T3   7075-T6

Test stress = 30 ksi, R = -1.   L-59-2088

Figure 9.- Photomicrographs of cracks in unloaded specimens.

$$LOG_{10} \, r = 0.00509 \, K_N S_{NET} - 5.472 - \frac{34}{K_N S_{NET} - 34}$$

S = 36.5 ksi

26.3

18.1

15.0 (CONSTANT STRESS)

W = 36 IN;
$\rho' = 0.002$ IN.

$K_N S_{NET}$, ksi

CRACK
PROPAGATION
RATE
IN./CYCLE

10^{-2}
10^{-3}
10^{-4}
10^{-5}
10^{-6}

200   400   600
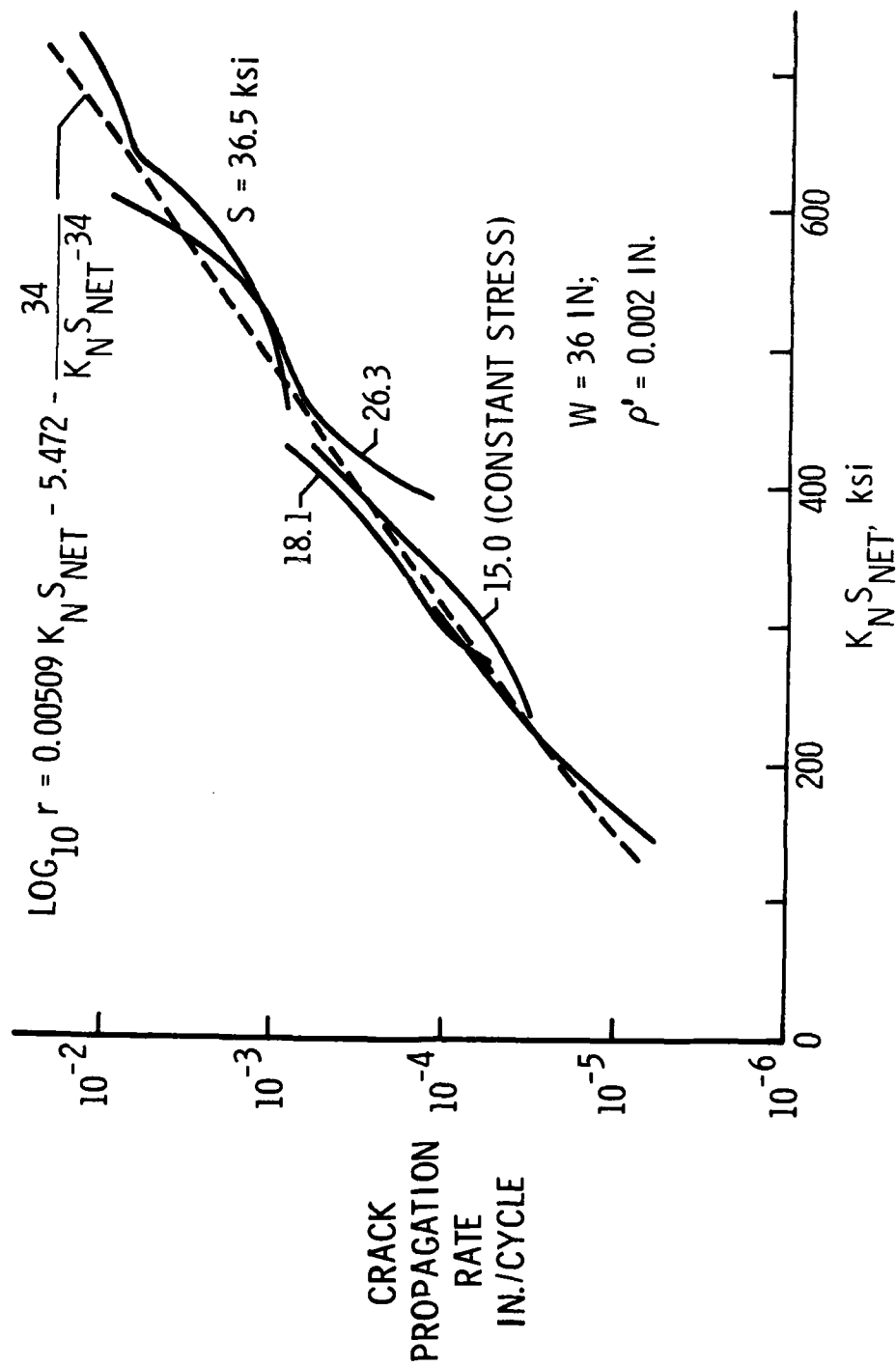
D.T.D. 5~6B aluminum alloy. R = 0.

Figure 10.- Fatigue crack propagation.
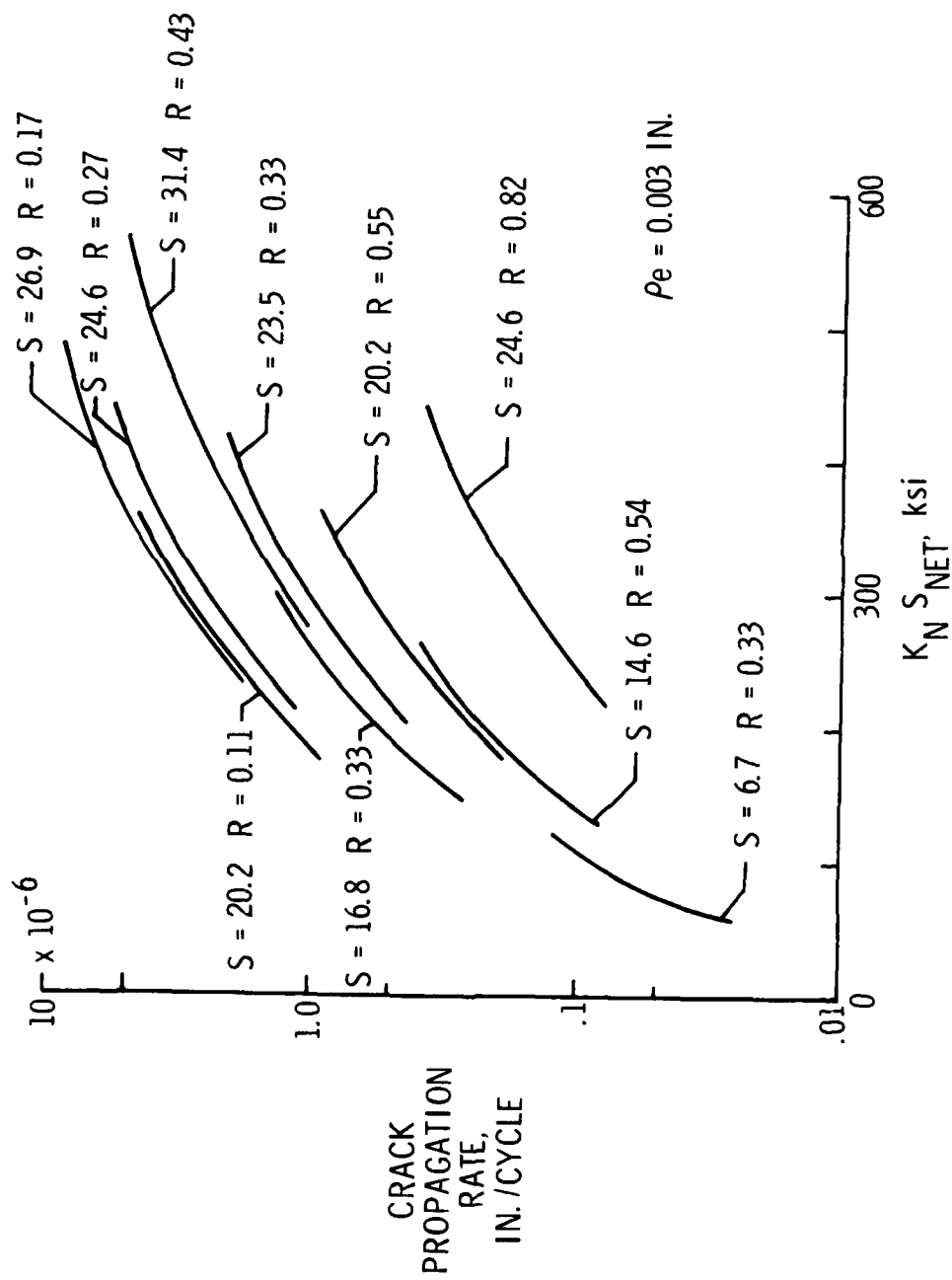
NASA

Figure 11.- Effect of R on crack propagation in mild steel.
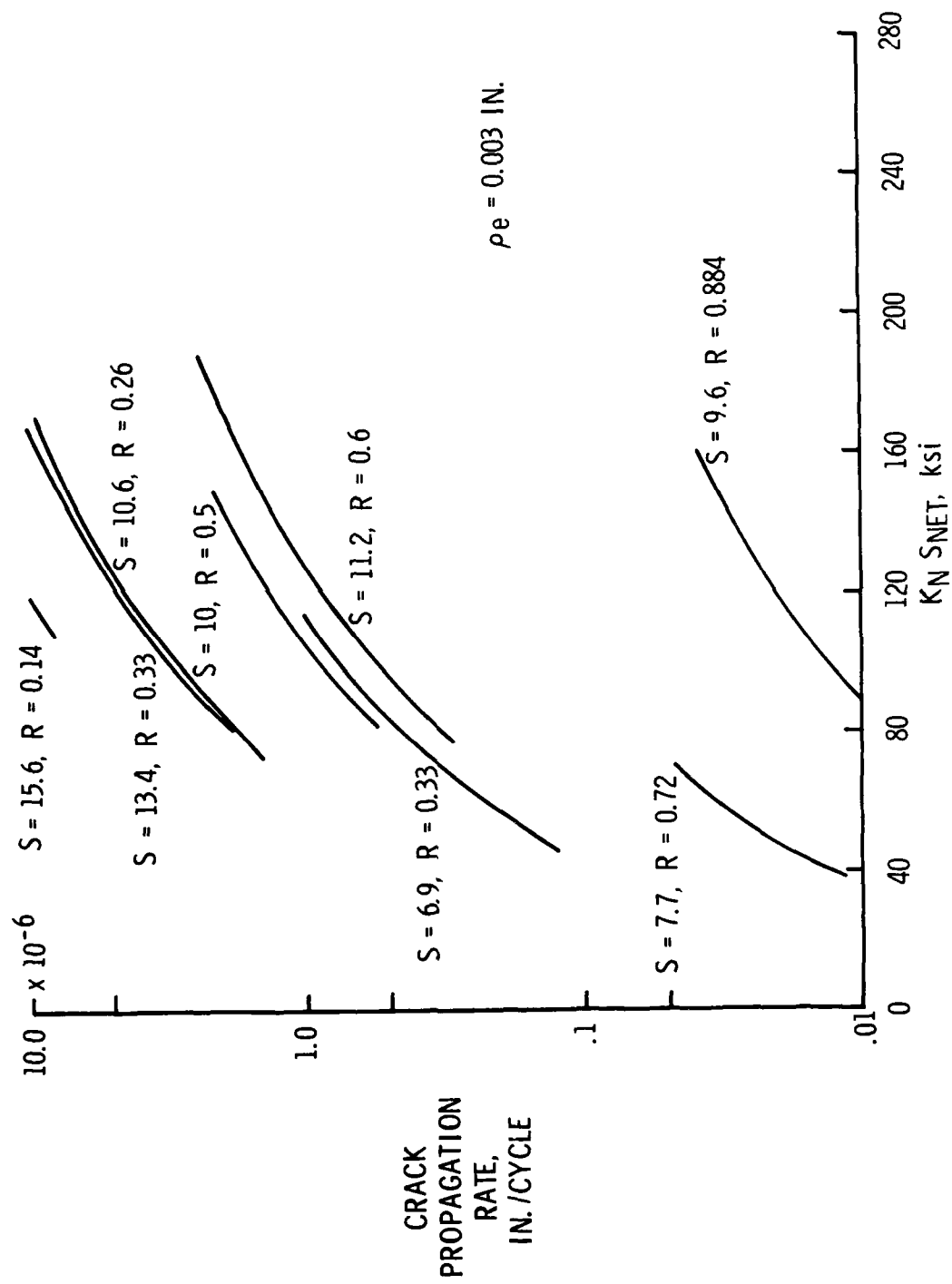
NASA

Figure 12.- Effect of R on crack propagation in aluminum alloy.
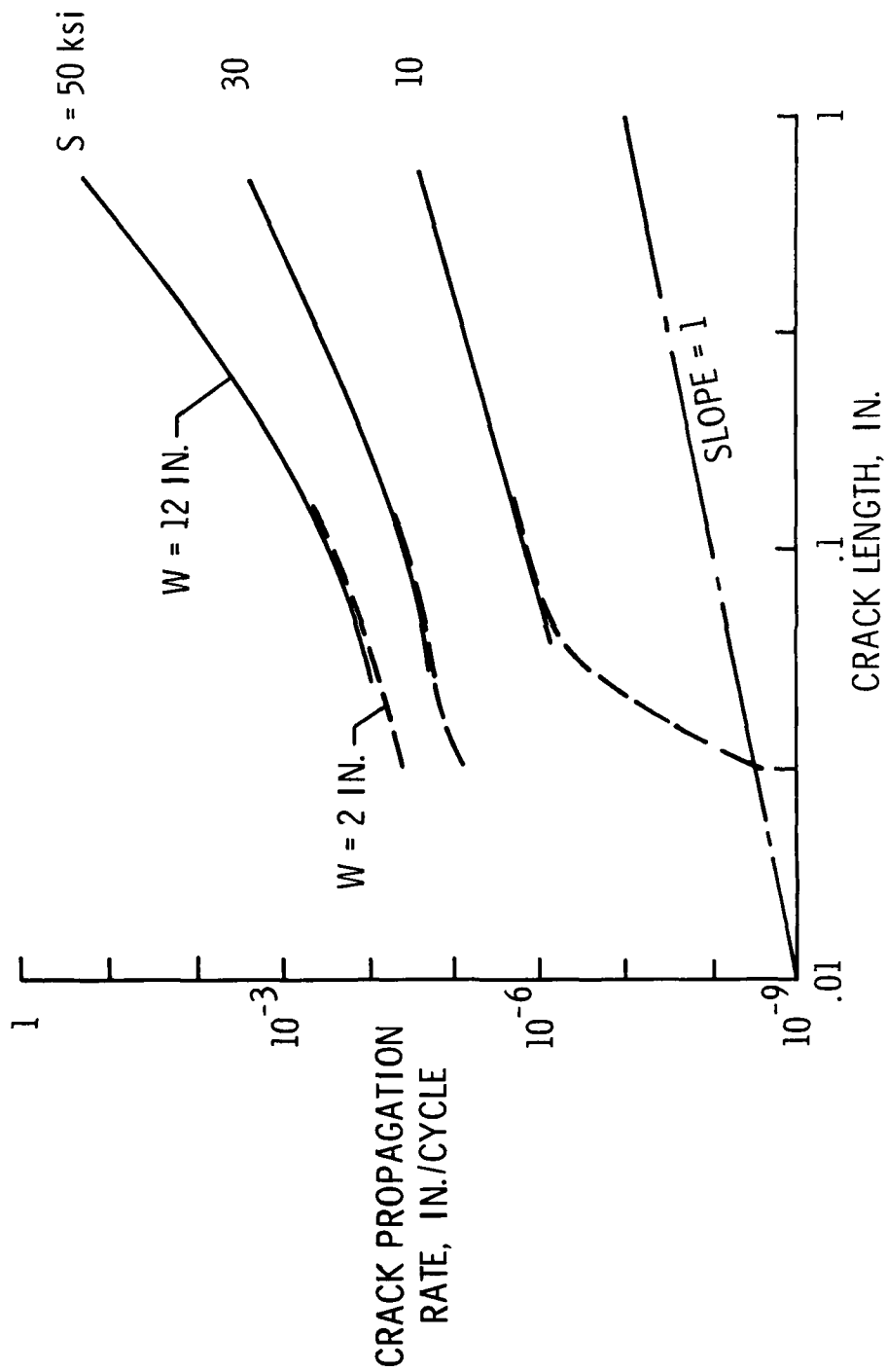
Figure 13.- Correlation with Frost method.
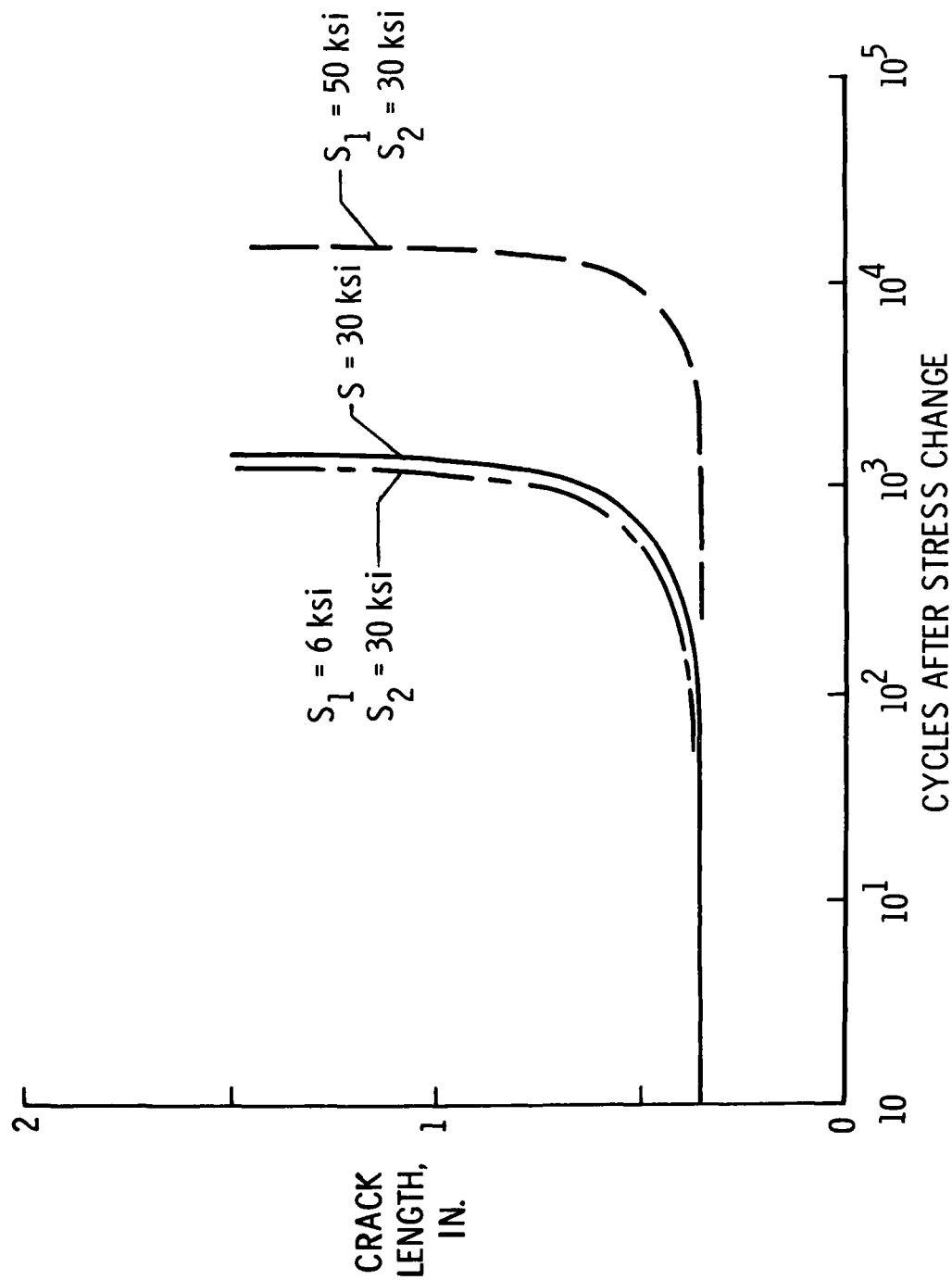
2024-T3 aluminum alloy, R = 0, W = 12 inches.

Figure 14.- Crack propagation in two-step test.

NASA
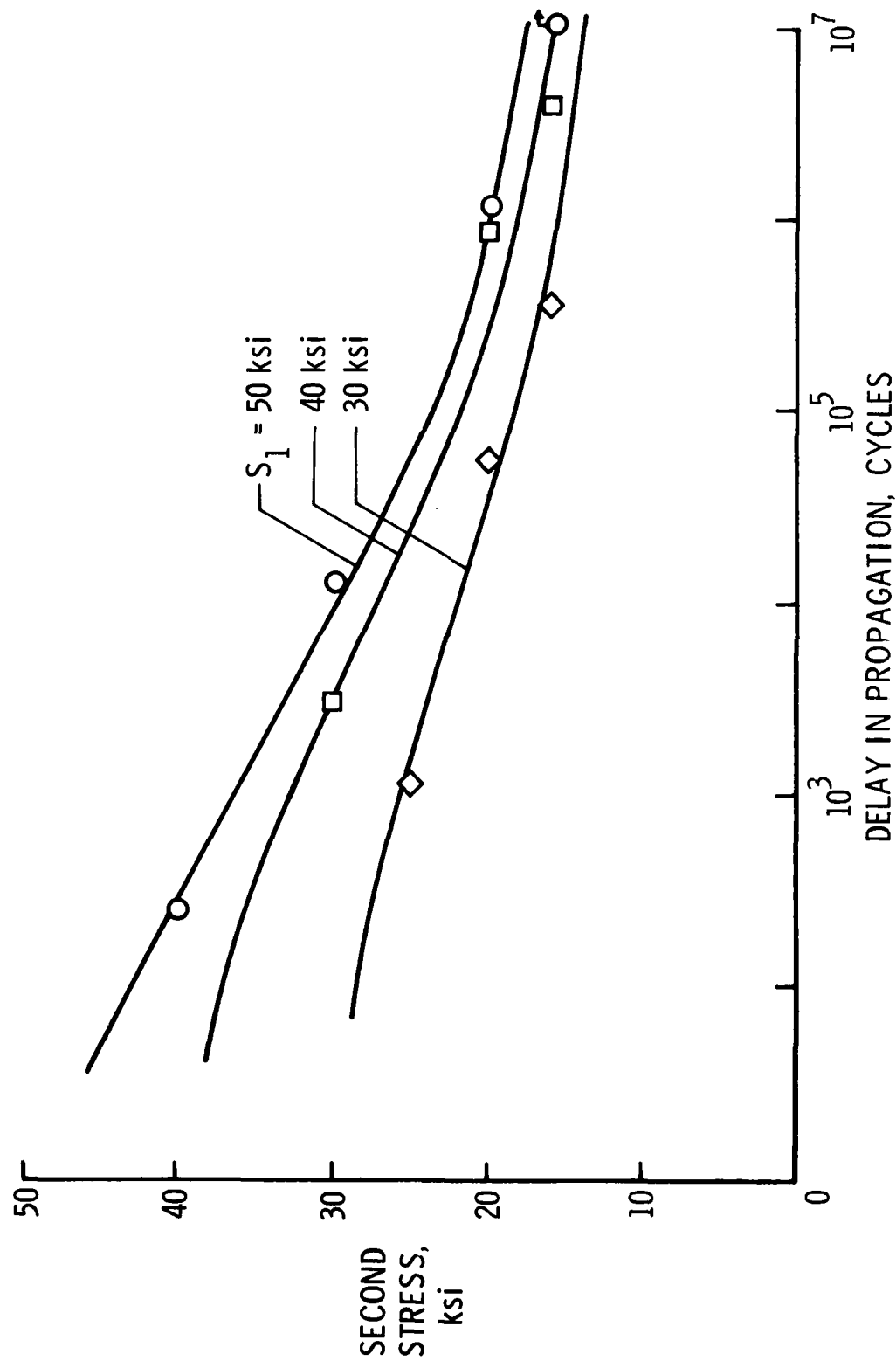
2024-T3 aluminum alloy, R = 0, W = 12 inches.

Figure 15.- Delay in crack propagation in two-step tests.
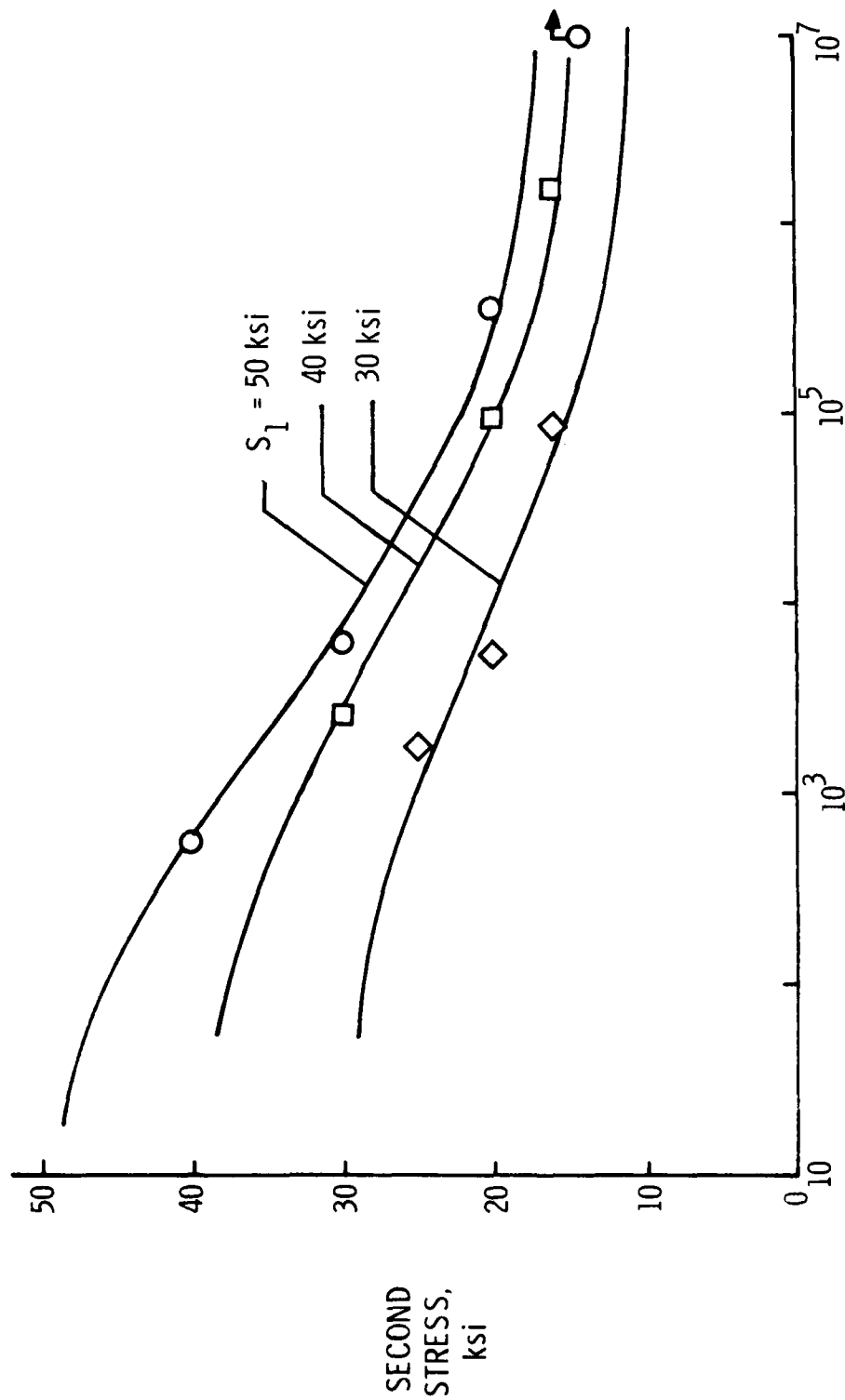
NASA

7075-T6 aluminum alloy, R = 0, W = 12 inches.

Figure 16.- Delay in crack propagation in two-step tests.
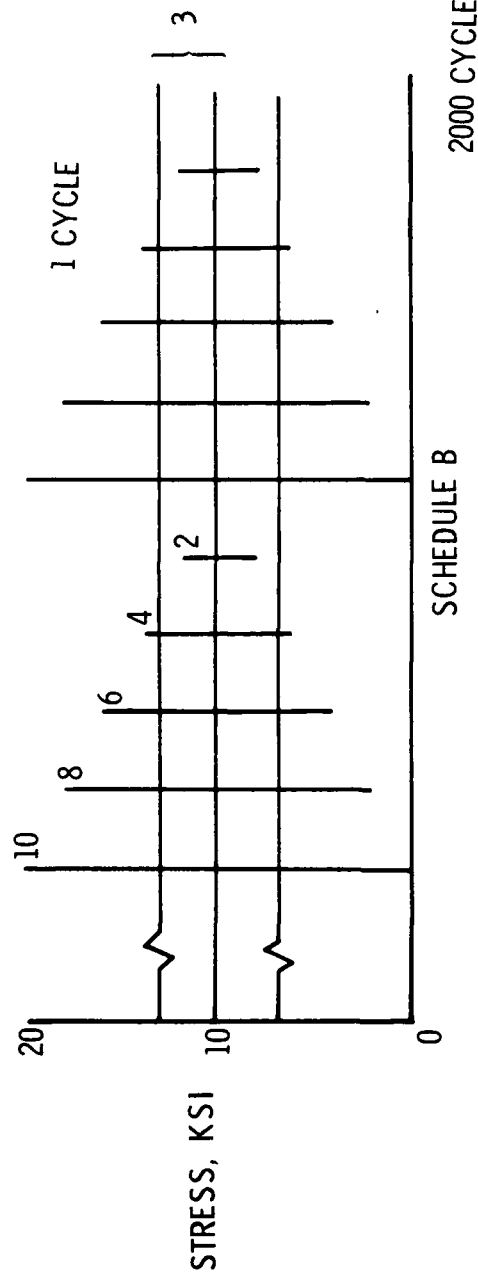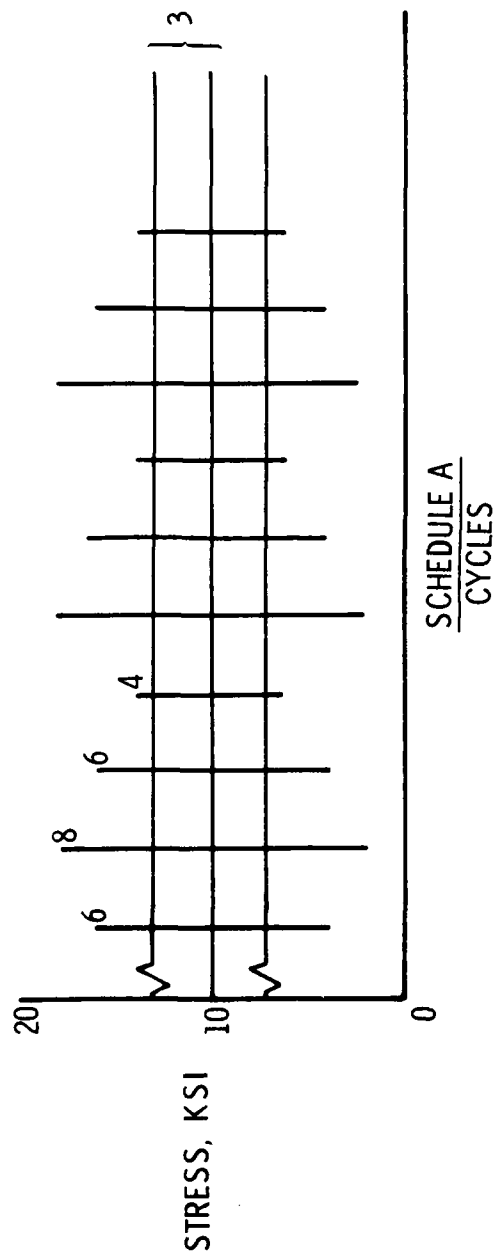
NASA

Figure 17.- Load schedules for tests of simulated spar caps.
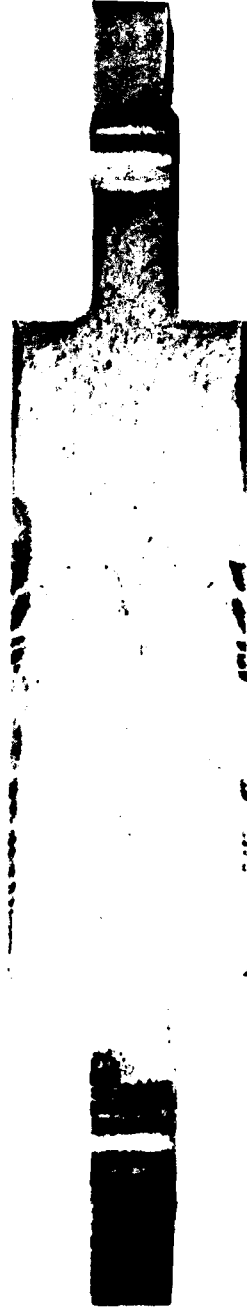
SPECIMEN A

SPECIMEN B

2024-T4 aluminum alloy.

Figure 18.- Fractographs of fatigue failures.

NASA

X7275-T6

7075-T6

.01 IN.

Figure 19.- Microstructure of two Al-Zn-Mg alloys.
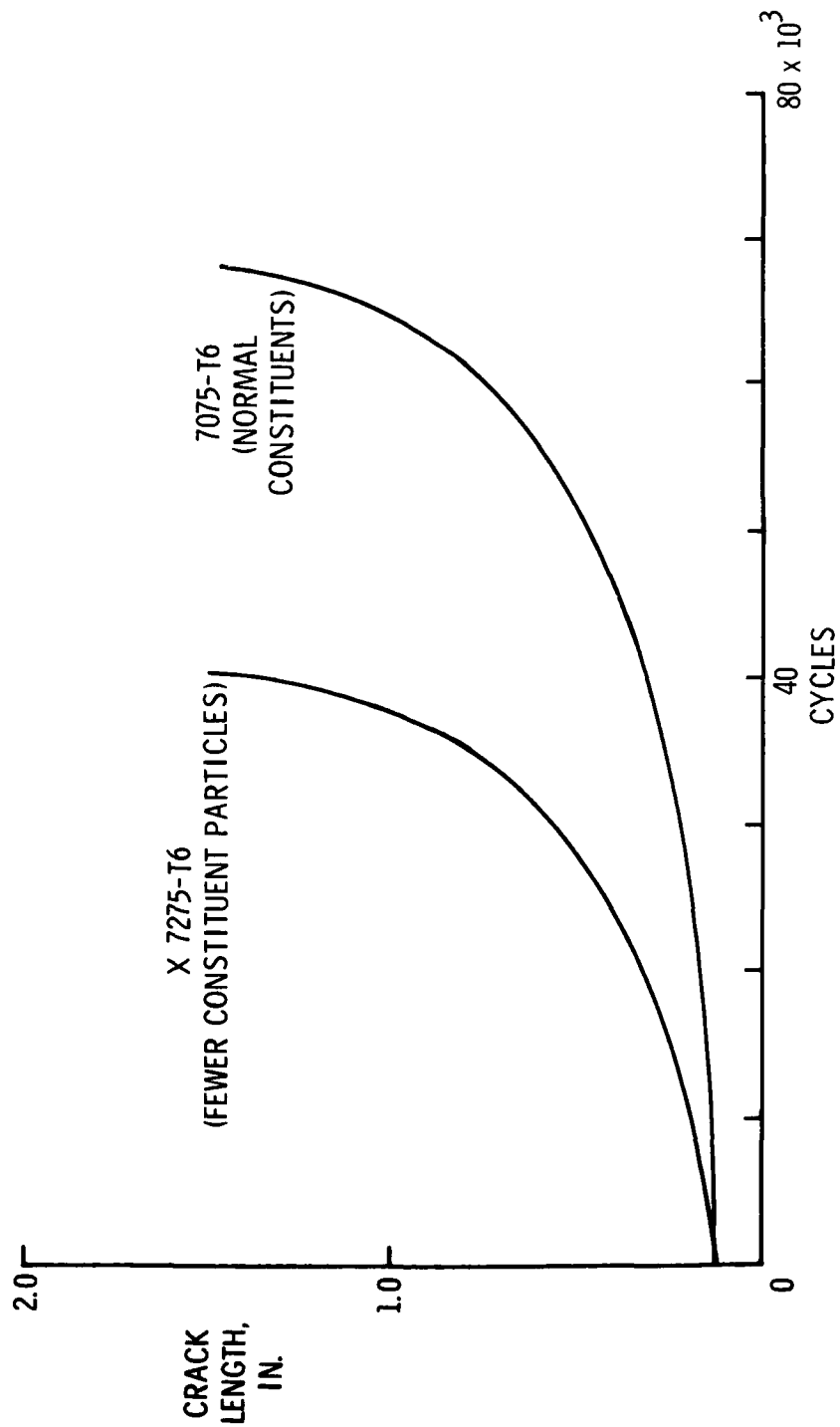
Figure 20.- Effect of constituent particles on fatigue crack propagation.
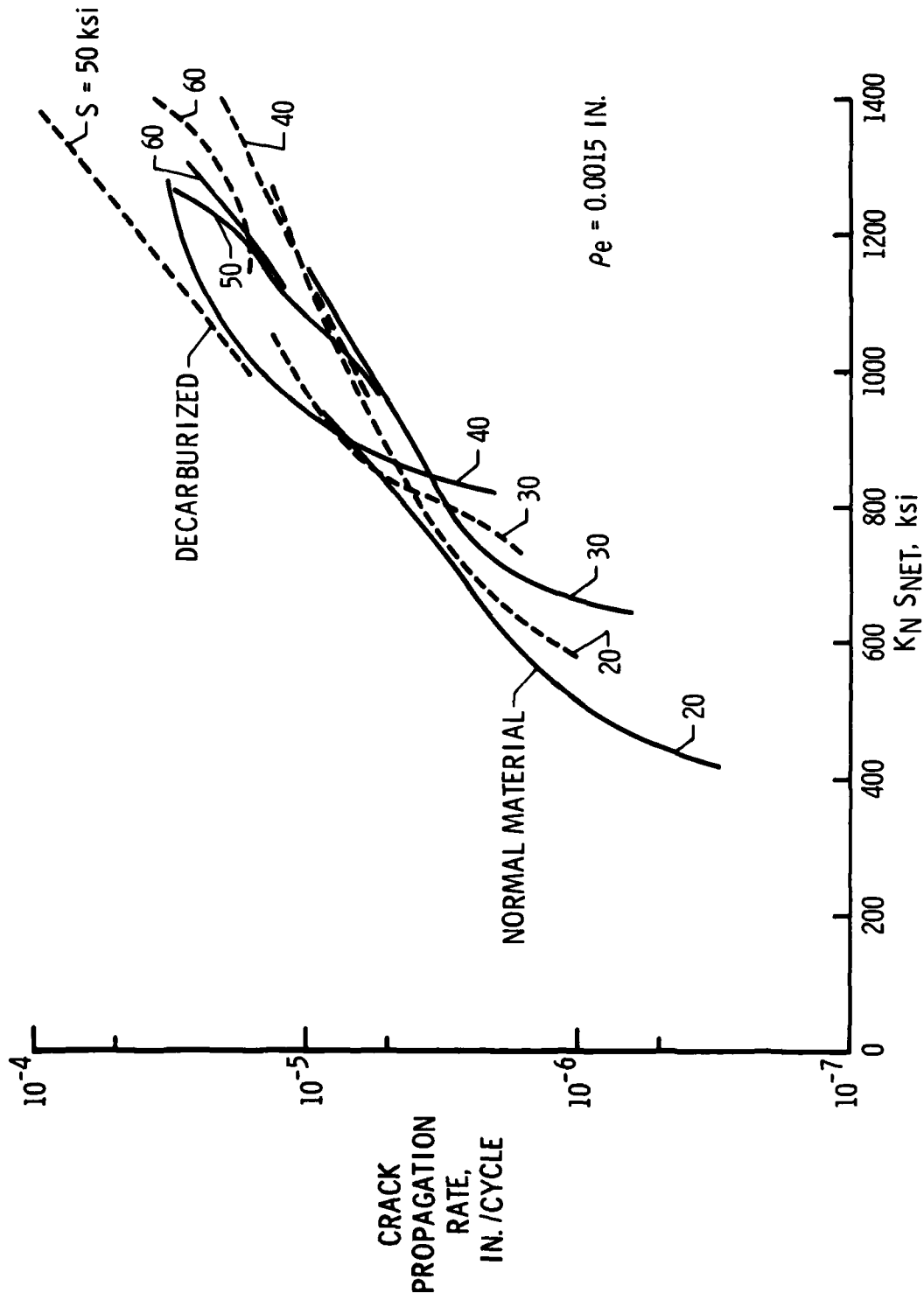
NASA

12 Mo V steel, $R = 0$, $W = 2$ inches.

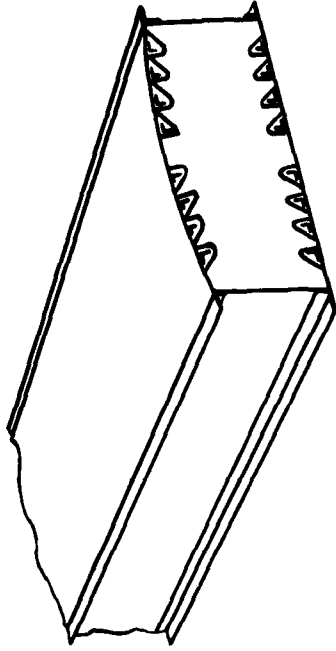Figure 21.- Effect of decarburization.
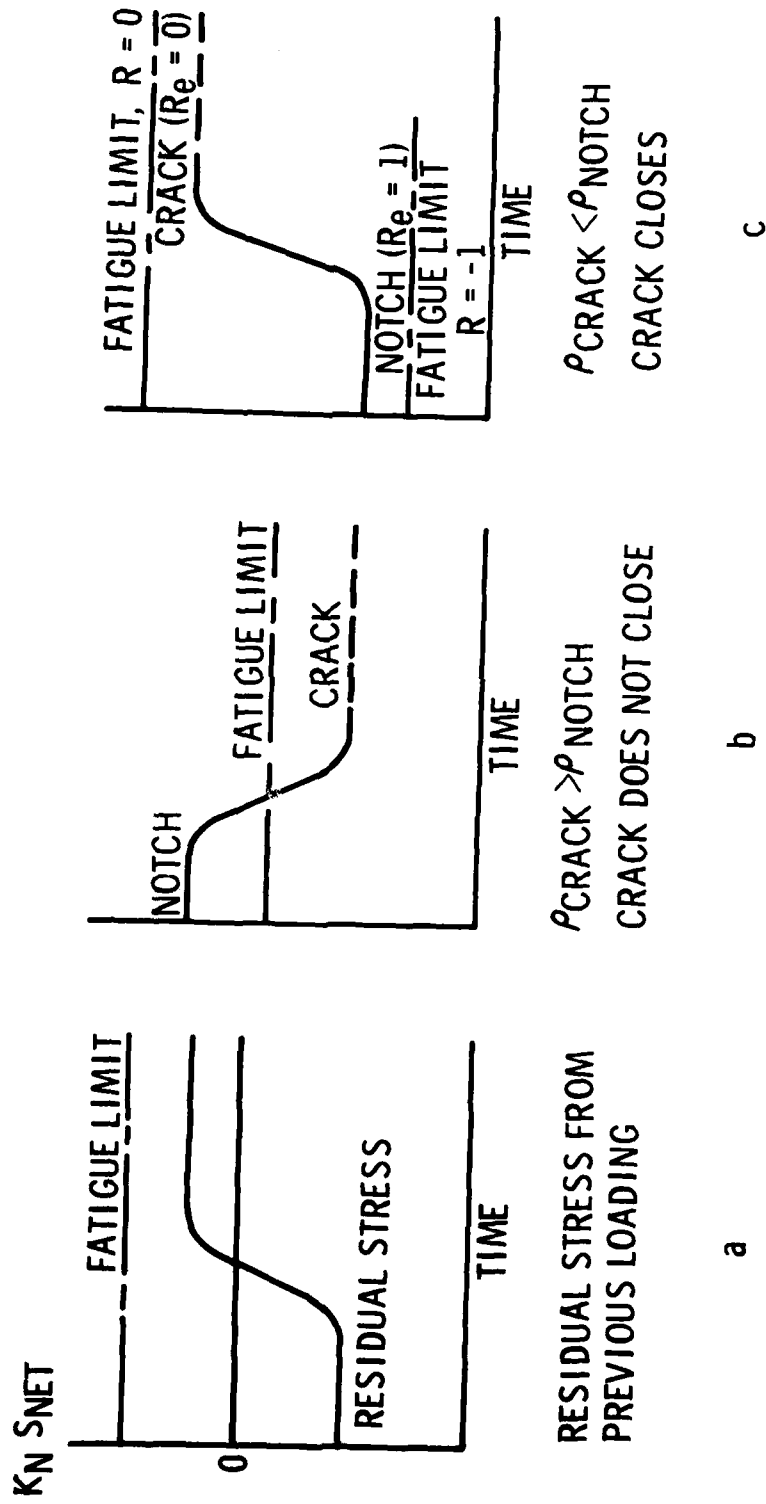
Figure 22.- Nonpropagating cracks.

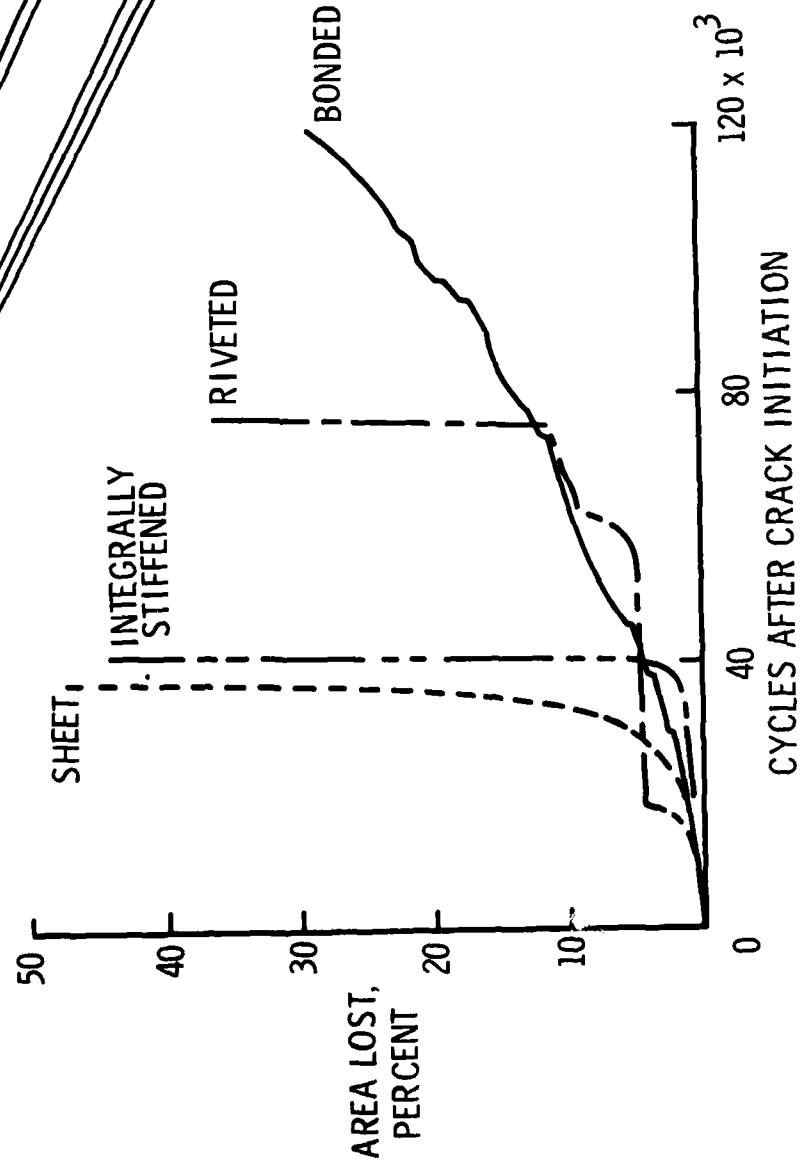$$S_0 = \frac{S_e}{1 + \frac{1}{2}(K_c - 1)\sqrt{\frac{l}{\rho_e}}}$$

$\rho_e = 0.016$ IN.

$S_0 l^3 = $ CONSTANT

CRITICAL
PROPAGATING
STRESS,
S_0, ksi
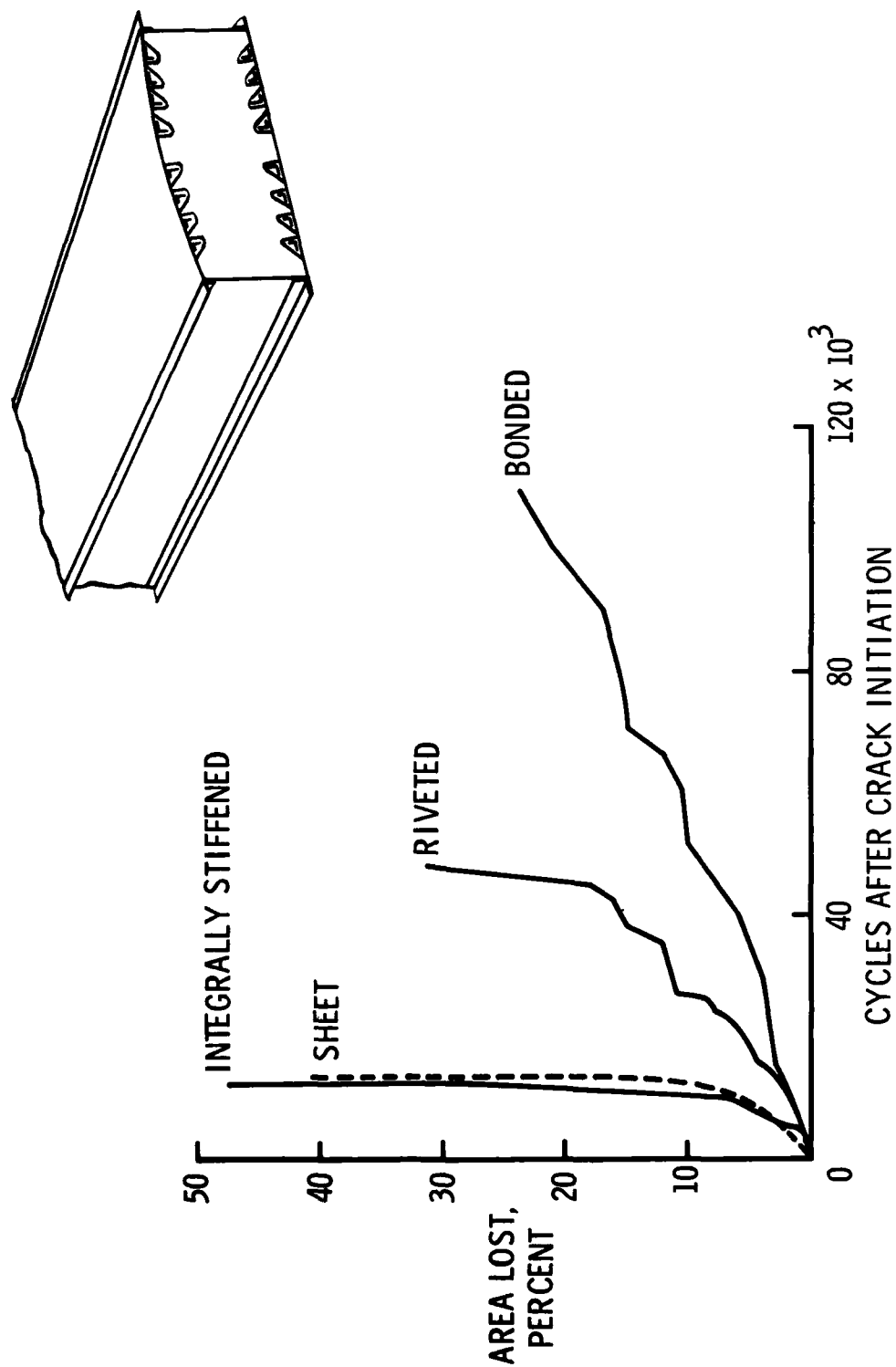
CRACK LENGTH, l, IN.
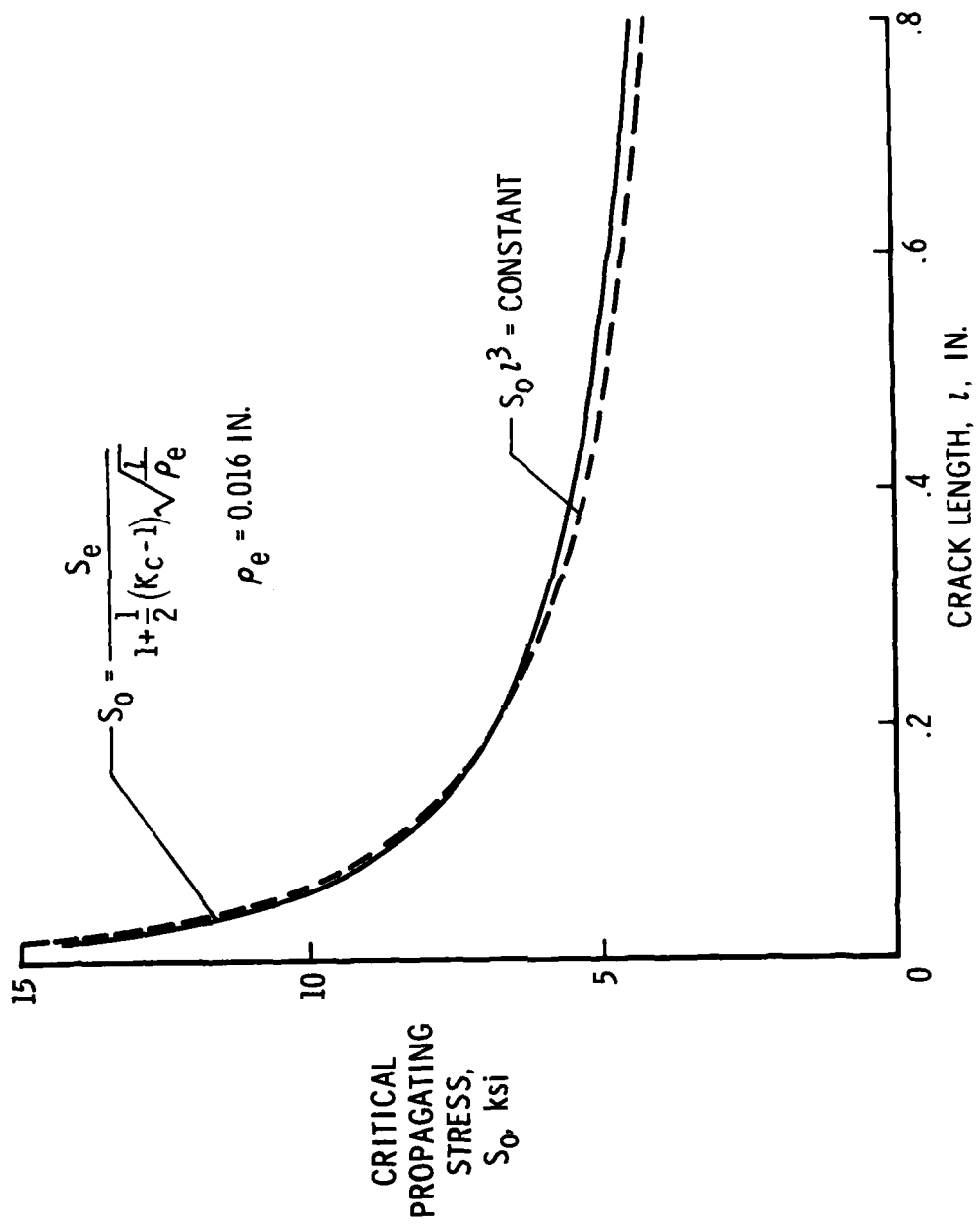
NASA

Figure 23.- Prediction of critical propagating stress.
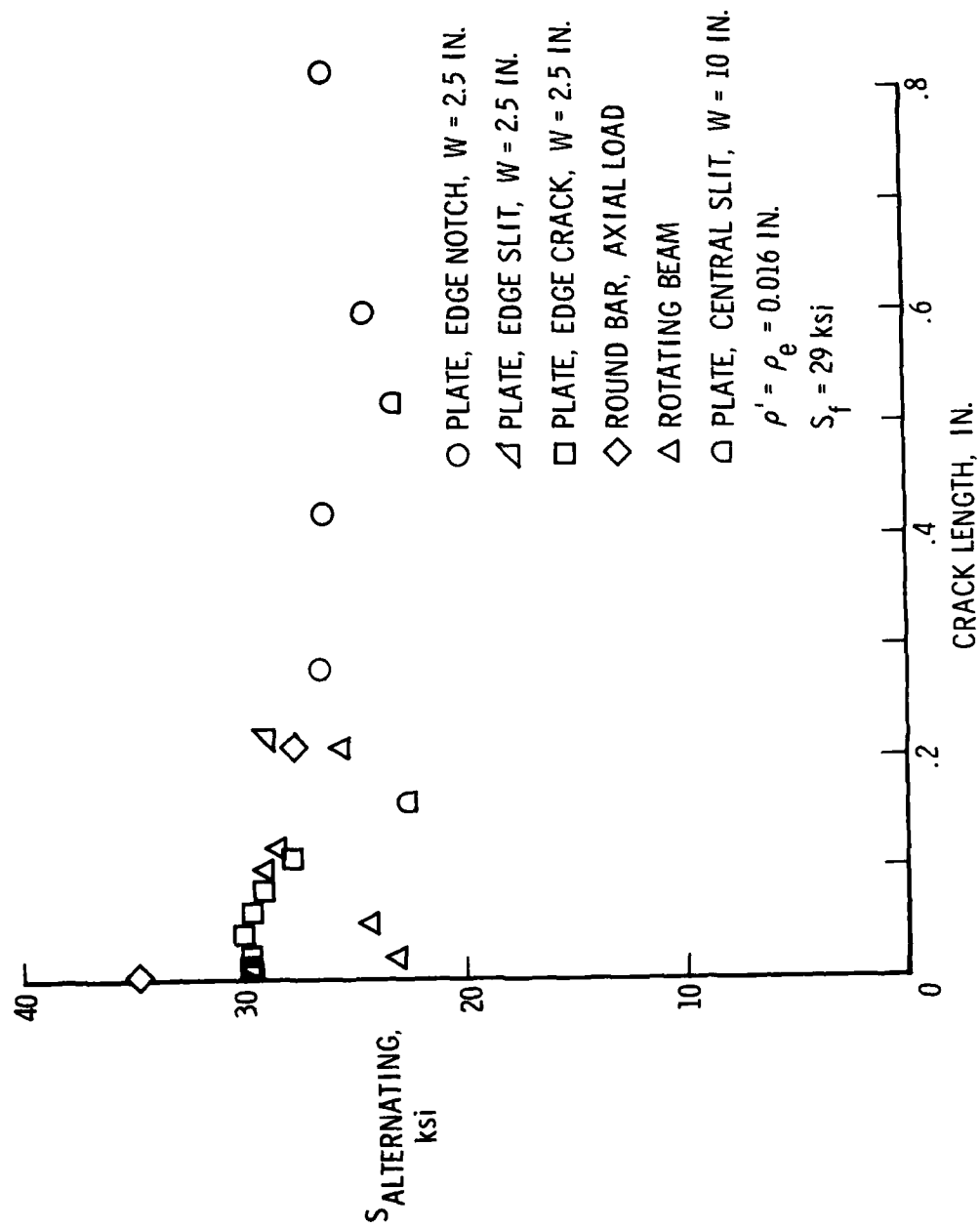
Figure 24.- Nonpropagating cracks in mild steel.

NASA

2024-T3 aluminum alloy S = 13 ± 6.5 ksi.

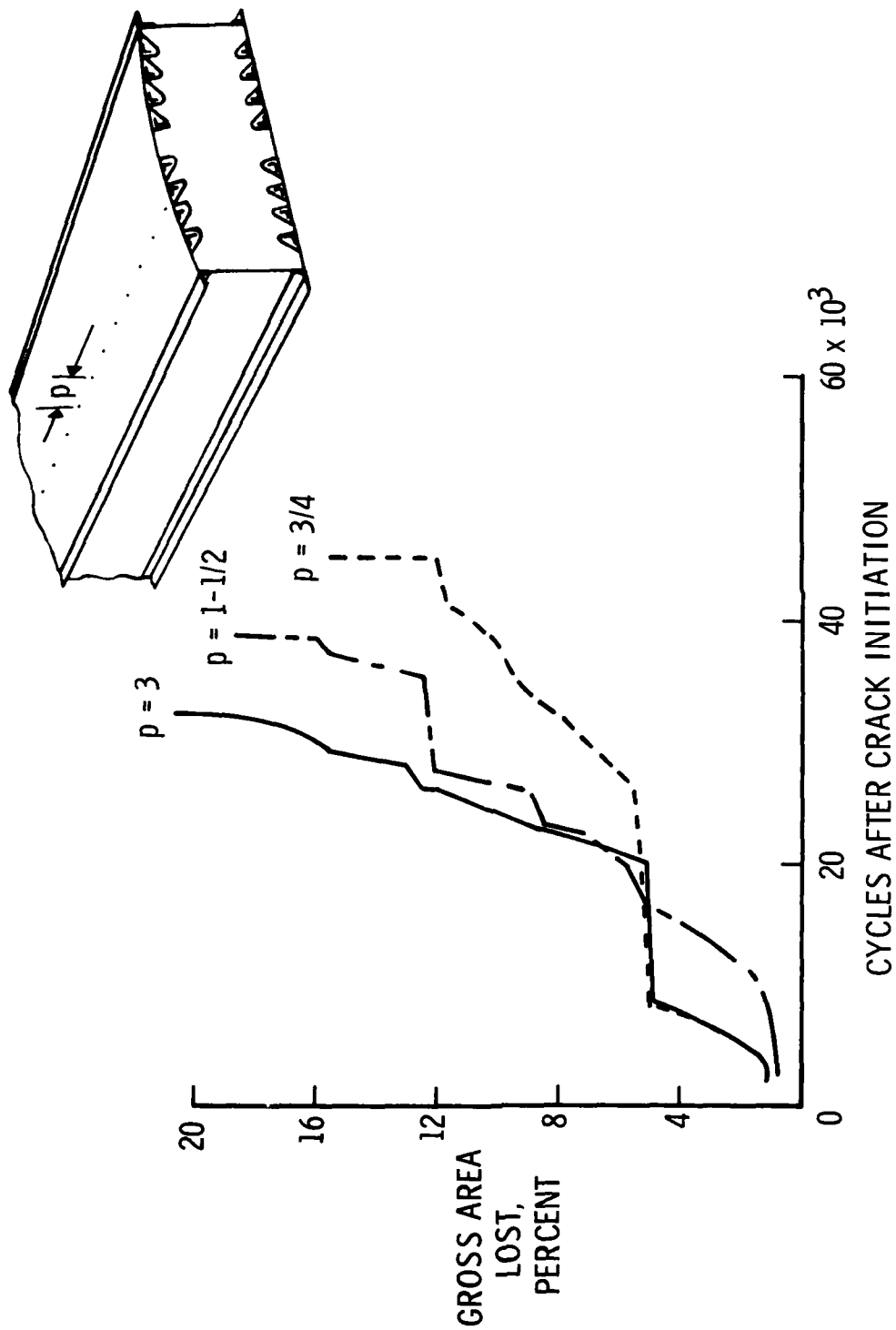Figure 25.- Crack propagation in box beams.

NASA

7075-T6 aluminum alloy, S = 13 ± 6.5 ksi.
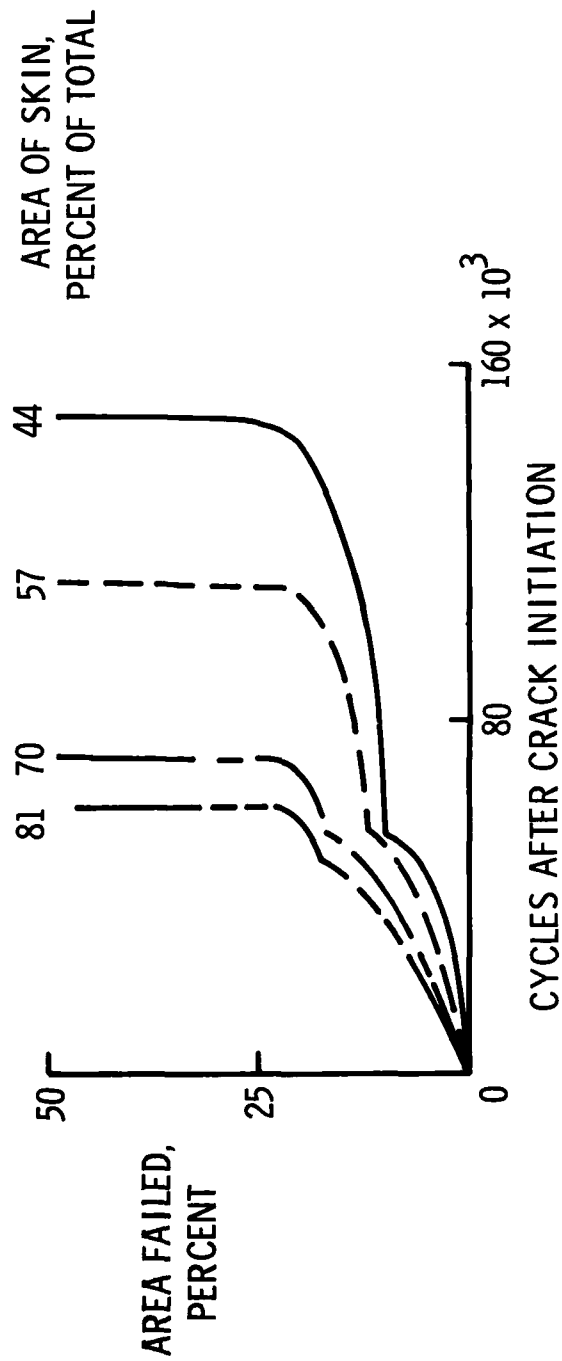
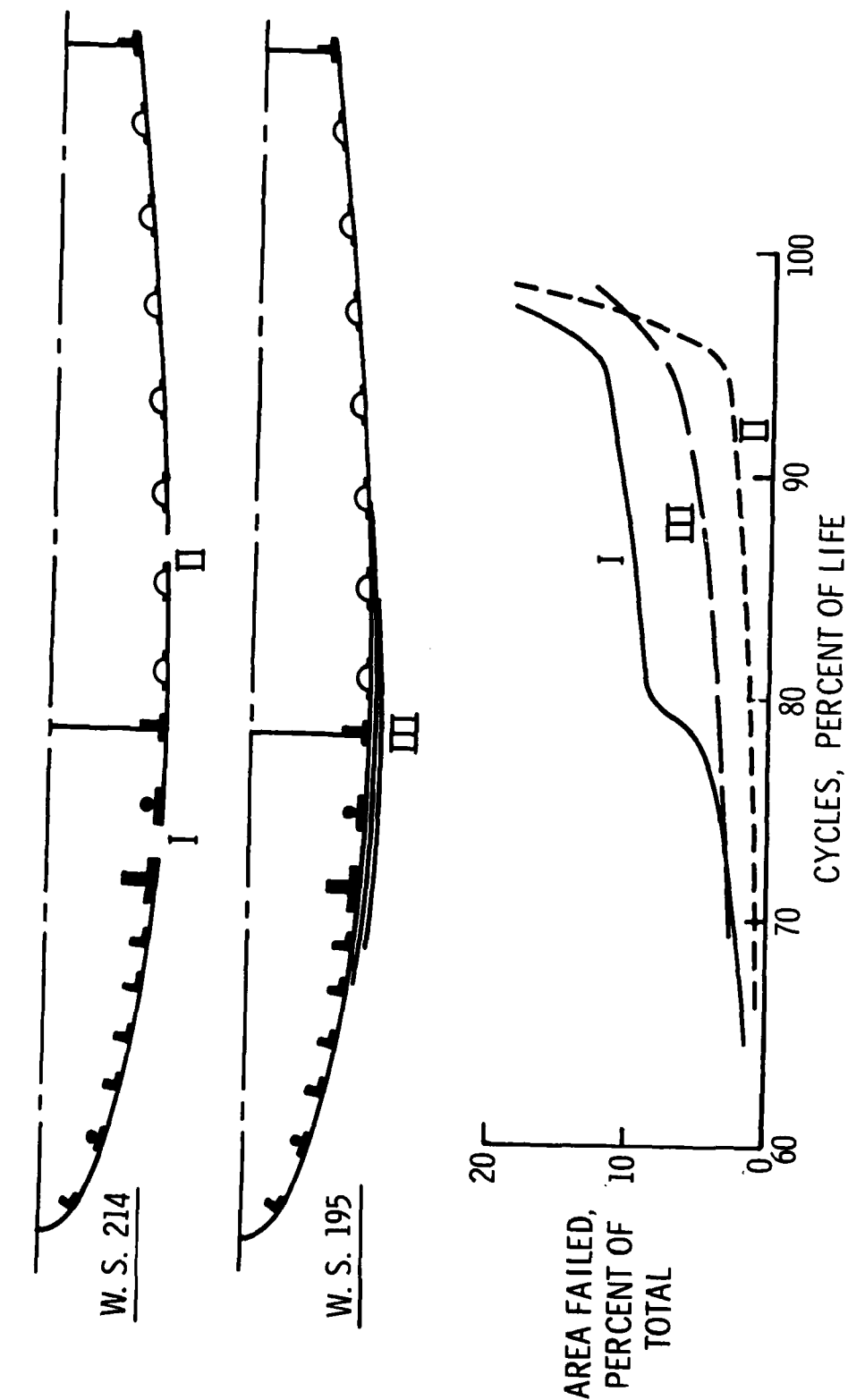Figure 26.- Crack propagation in box beams.

NASA

GROSS AREA LOST, PERCENT

CYCLES AFTER CRACK INITIATION

p = 3

p = 1-1/2

p = 3/4

60 x 10³

7075-T6 aluminum alloy, S = 13 ± 6.5 ksi.

Figure 27.- Effect of rivet pitch on crack propagation in box beams.

NASA

AREA OF SKIN,
PERCENT OF TOTAL

CYCLES AFTER CRACK INITIATION

2024-T3 aluminum alloy, S = 14 ± 4.7 ksi.

Figure 28.- Crack propagation in stiffened panels.

NASA

Figure 29.- Crack propagation in C-46 wings.

W.S. 214

W.S. 195

AREA FAILED, PERCENT OF TOTAL

CYCLES, PERCENT OF LIFE

NASA